Contrib Mineral Petrol (2005) 150: 608–630
DOI 10.1007/s00410-005-0038-3

ORIGINAL PAPER

Anthi Liati

Identification of repeated Alpine (ultra) high-pressure metamorphic events by U–Pb SHRIMP geochronology and REE geochemistry of zircon: the Rhodope zone of Northern Greece

Received: 17 March 2005 / Accepted: 19 September 2005 / Published online: 8 November 2005

Abstract U–Pb sensitive high resolution ion microprobe (SHRIMP) zircon geochronology, combined with REE geochemistry, has been applied in order to gain insight into the complex polymetamorphic history of the (ultra) high pressure [(U)HP] zone of Rhodope. Dating included a paragneiss of Central Rhodope, for which (U)HP conditions have been suggested, an amphibolitized eclogite, as well as a leucosome from a migmatized orthogneiss at the immediate contact to the amphibolitized eclogite, West Rhodope. The youngest detrital zircon cores of the paragneiss yielded ca. 560 Ma. This date indicates a maximum age for sedimentation in this part of Central Rhodope. The concentration of detrital core ages of the paragneiss between 670–560 Ma and around 2 Ga is consistent with a Gondwana provenance of the eroded rocks in this area of Central Rhodope. Metamorphic zircon rims of the same paragneiss yielded a lower intercept $^{206}Pb/^{238}U$ age of 148.8 ± 2.2 Ma. Variable post-148.8 Ma Pb-loss in the outermost zircon rims of the paragneiss, in combination with previous K–Ar and SHRIMP-data, suggest that this rock of Central Rhodope underwent an additional Upper Eocene (ca. 40 Ma) metamorphic/fluid event. In West Rhodope, the co-magmatic zircon cores of the amphibolitized eclogite yielded a lower intercept $^{206}Pb/^{238}U$ age of 245.6 ± 3.9 Ma, which is interpreted as the time of crystallization of the gabbroic protolith. The metamorphic zircon rims of the same rock gave a lower intercept $^{206}Pb/^{238}U$ age of 51.0 ± 1.0 Ma. REE data on the metamorphic rims of the zircons from both the paragneiss of Central Rhodope and the amphibolitized eclogite of West Rhodope show no Eu anomaly in the chondrite-normalized patterns, indicating that they formed at least under HP conditions. Flat or nearly flat HREE profiles of the same zircons are consistent with the growth of garnet at the time of zircon formation. Low Nb and Ta contents of the zircon rims in the amphibolitized eclogite indicate concurrent growth of rutile. Based on the REE characteristics, the 148.8 ± 2.2 Ma age of the garnet–kyanite paragneiss, Central Rhodope and the 51.0 ± 1.0 Ma age of the amphibolitized eclogite, West Rhodope are interpreted to reflect the time close to the (U)HP and HP metamorphic peaks, respectively, with a good approximation. The magmatic zircon cores of the leucosome in the migmatized orthogneiss, West Rhodope, gave a lower intercept $^{206}Pb/^{238}U$ age of 294.3 ± 2.4 Ma for the crystallization of the granitoid protolith of the orthogneiss. Two oscillatory zircon rims around the Hercynian cores, yielded ages of 39.7 ± 1.2 and 38.1 ± 0.8 Ma (2σ errors), which are interpreted as the time of leucosome formation during migmatization. The zircons in the leucosome do not show the 51 Ma old HP metamorphism identified in the neighboring amphibolitized eclogite, possibly because the two rock types were brought together tectonically after 51 Ma. If one takes into account the two previously determined ages of ca. 73 Ma for (U)HP metamorphism in East Rhodope, as well as the ca. 42 Ma for HP metamorphism in Thermes area, Central Rhodope, four distinct events of (U)HP metamorphism throughout Alpine times can be distinguished: 149, 73, 51 and 42 Ma. Thus, it is envisaged that the Rhodope consists of different terranes, which resulted from multiple Alpine subductions and collisions of micro-continents, rather similar to the presently accepted picture in the Central and Western Alps. It is likely that these microcontinents were rifted off from thinned continental margins of Gondwana, between the African and the European plates before the onset of Alpine convergence.

Communicated by W. Schreyer

A. Liati
Institute of Isotope Geology and Mineral Resources,
Swiss Federal Institute of Technology (ETH),
Sonneggstrasse 5, 8092 Zurich, Switzerland
E-mail: liati@erdw.ethz.ch

Introduction

(Ultra) high pressure [(U)HP] polymetamorphic terranes of mountain belts are usually involved into a fairly

complex geological history. Reliable geochronological data are an indispensable tool for unravelling their complex tectonometamorphic evolution. However, absolute age determination of distinct geologic events e.g., age of sedimentation, magmatism, metamorphism(s), in complex orogens is a difficult task. Geochronological data obtained by commonly used isotopic systems (e.g., Rb–Sr, K–Ar, Ar–Ar, Sm–Nd, Lu–Hf, U–Pb) relying on mineral separates, whole rocks or minerals showing multiple growth/recrystallization domains (e.g., garnet, mica, composite zircon crystals) and/or containing inclusions are problematic and often geologically inconclusive (see e.g., summary by Gebauer 1999 and references therein; Rubatto et al. 2003 and references therein). The most common problem with many geochronometers is that they mainly rely on the preservation of only local equilibrium within the same rock sample, due to micrometer-small heterogeneities. There is, therefore, a necessity of analyzing micrometer-large parts of minerals in order to obtain reliable age results from these complex systems. The sensitive high resolution ion microprobe (SHRIMP) dating method of the mineral zircon fulfils this requirement and is a powerful technique, more than any other dating technique currently available, to obtain reliable age data for the metamorphic events, the protolith and the sedimentation time of rocks involved in complex orogenic processes. Thus, SHRIMP geochronology in the Western and Central Alps, for instance, led to a substantial revision of ideas concerning its geodynamic evolution (see Gebauer 1999, for a summary).

Within the framework of the present paper, the U–Pb SHRIMP technique was applied in order to date different rock types from the (U)HP zone of Rhodope in Northern Greece. The Rhodope zone, which extends within Southern Bulgaria and Northern Greece, represents a stack of metamorphic thrust sheets recording a long history of Alpine orogenic deformation (e.g., Burchfiel 1980; Liati 1986; Burg et al. 1990; Dinter and Royden 1993). Based on previous work, HP and in parts (U)HP metamorphism has affected the Rhodope (e.g., Liati 1986; Kolceva 1986; Mposkos 1989; Liati and Seidel 1996; Mposkos and Kostopoulos 2001; Liati et al. 2002).

The aim of this paper is to investigate the time of metamorphic events and of protolith formation (sedimentation and magmatism) in parts of Central and West Rhodope. In Central Rhodope, a garnet–kyanite (grt–ky) paragneiss was dated. For this rock type, microdiamonds, and therefore (U)HP conditions, have been suggested by Mposkos and Kostopoulos (2001). In West Rhodope, an amphibolitized eclogite, as well as the leucosome from a migmatized orthogneiss at the immediate contact to the amphibolitized eclogite, were included for dating. With the exception of some scattering Ar-data (Liati 1986; Liati and Kreuzer 1990), no metamorphic or magmatic ages are reported for West Rhodope, so far. Hence, the SHRIMP-data presented in this work are the first age data constraining the time of HP metamorphism and pre-metamorphic magmatism. In order to better limit the link between SHRIMP-ages and conditions of metamorphism, under which the metamorphic zircon domains formed, the REE composition of the same metamorphic zircon domains that were dated for their U–Pb SHRIMP-age was determined by means of LA-ICPMS and SHRIMP II. Zircons from an amphibolitized kyanite–eclogite in Central Rhodope dated previously by SHRIMP (Liati and Gebauer 1999) were also included in the REE study. The geochronological data, in combination with the REE geochemical data, aim to further contribute to the reconstruction of the geodynamic evolution of this orogen.

Overview and geological setting of the Rhodope

The Rhodope zone is situated between the Balkan belt to the north and the Dinarides-Hellenides to the SSW, at the eastern part of the European Alpine orogen (Fig. 1). A low-angle normal fault, related to Late Miocene/Late Pliocene extension, separates the Rhodope from the neighboring Serbomacedonian Massif to the west (Dinter and Royden 1993). Based on similarities in metamorphic grade and structural style, the Rhodope and the Serbomacedonian are viewed by some authors

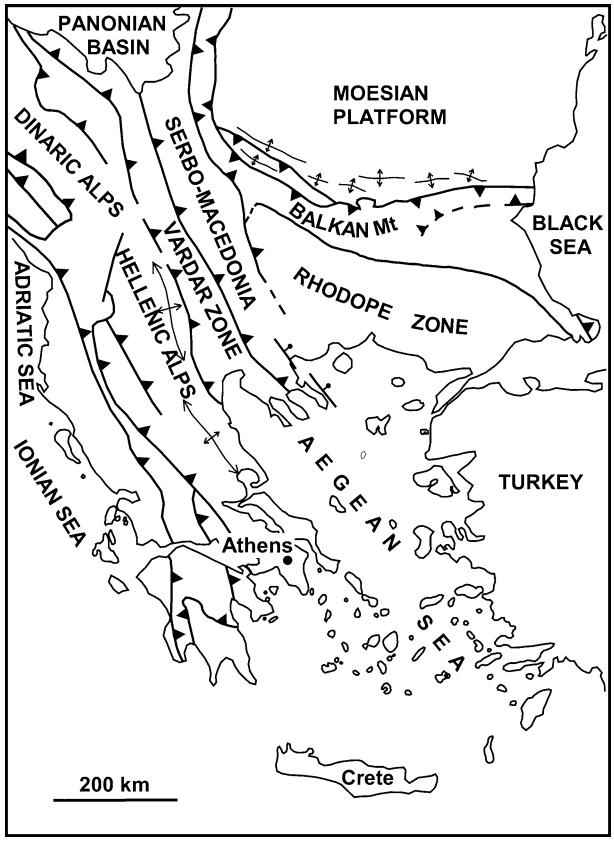

Fig. 1 Sketch map of major tectonic elements in southeastern Europe and the northeastern Mediterranean region (from Burchfiel 1980; Dinter et al. 1995)

as a single tectonic element (e.g., Burg et al. 1995). Both Rhodope and Serbomacedonian Massif lie east of the Vardar zone, which is interpreted as a Mid–Late Mesozoic oceanic suture between Apulia and the SE European margin.

The Rhodope consists of a series of distinct tectonic units comprising both oceanic and continental metamorphic rocks intruded and overlain by post-metamorphic plutonic and volcanic rocks. The metamorphic rocks show widespread amphibolite-facies and locally granulite-facies metamorphism, while some of them (mainly the basic lithologies) preserve relics of a previous eclogite-facies (e.g., Liati 1986; Kolceva et al. 1986; Mposkos 1989; Liati and Seidel 1996). (U)HP metamorphism was recently reported in parts of Eastern and Central Rhodope (Liati and Gebauer 2001a; Mposkos and Kostopoulos 2001; Liati et al. 2002).

Various authors have proposed several basic schemes for a subdivision of Rhodope into different units (e.g., Papanikolaou and Panagopoulos 1981; Mposkos 1989; Burg et al. 1996). Tectonic data are relatively limited in the Rhodope, so that correlations of these tectonic units within the Greek part, but also between the Greek and the Bulgarian part, are relatively unclear. A commonly used distinction for the Greek part of Rhodope is the one introduced for the western and central Rhodope by Papanikolaou and Panagopoulos (1981), who proposed an upper unit (also known as Sidironero unit) and a lower one (also known as Pangaeo unit), separated by a SSE–NNW striking thrust plane. Mposkos (1989) suggested principally the same scheme, based on the abrupt change of metamorphic grade between the two units. He distinguished an upper tectonic unit of high temperature eclogite-facies metamorphism overprinted under medium- to upper-amphibolite-facies from a lower tectonic unit of low temperature eclogite-facies metamorphism overprinted at the upper greenschist- to lower-amphibolite-facies (corresponding to the Sidironero Unit and the Pangaeo unit of Papanikolaou and Panagopoulos 1981, respectively). Burg et al. (1995, 1996) suggested a subdivision of the whole Rhodope (including both the Greek and the Bulgarian part) into two major thrust domains, a 'lower terrane' and an 'upper terrane', representing the crystalline footwall and hanging wall of a crustal-scale duplex. Several intermediate terranes (thrust units) are stacked between the 'upper' and 'lower terrane'. A more recent scheme referring to the Bulgarian part of Central Rhodope suggests the presence of a dome structure with gently dipping detachment faults and asymmetric graben depressions interpreted as a 'metamorphic core complex', which resulted from orogenic collapse during exhumation (see e.g., Burg et al. 1996 and references therein; Ivanov 2000).

The areas chosen for the present study belong to the upper tectonic unit in the sense of Papanikolaou and Panagopoulos (1981) and Mposkos (1989) or to the intermediate terranes in the sense of Burg et al. (1995, 1996) (Fig. 2).

Previous geochronology of metamorphic rocks in the Rhodope

The problem of determining the ages of metamorphic events in the Rhodope has been originally approached by the K–Ar technique on micas and hornblendes. The disadvantage with this technique is that in rocks with a high-pressure history, K–Ar ages commonly show wide scattering with a tendency to erroneously high apparent ages caused by excess argon. This has been substantiated by numerous examples worldwide (e.g., Kelley 2002 and references therein; Gebauer 1999). Nevertheless, a series of Ar-geochronological studies on metamorphic rocks of Rhodope (e.g., Liati 1986; Liati and Kreuzer 1990; Lips et al. 2000), despite their scattering, clearly showed a widespread Tertiary metamorphism. In the Greek part of Central Rhodope, K–Ar data on metamorphic

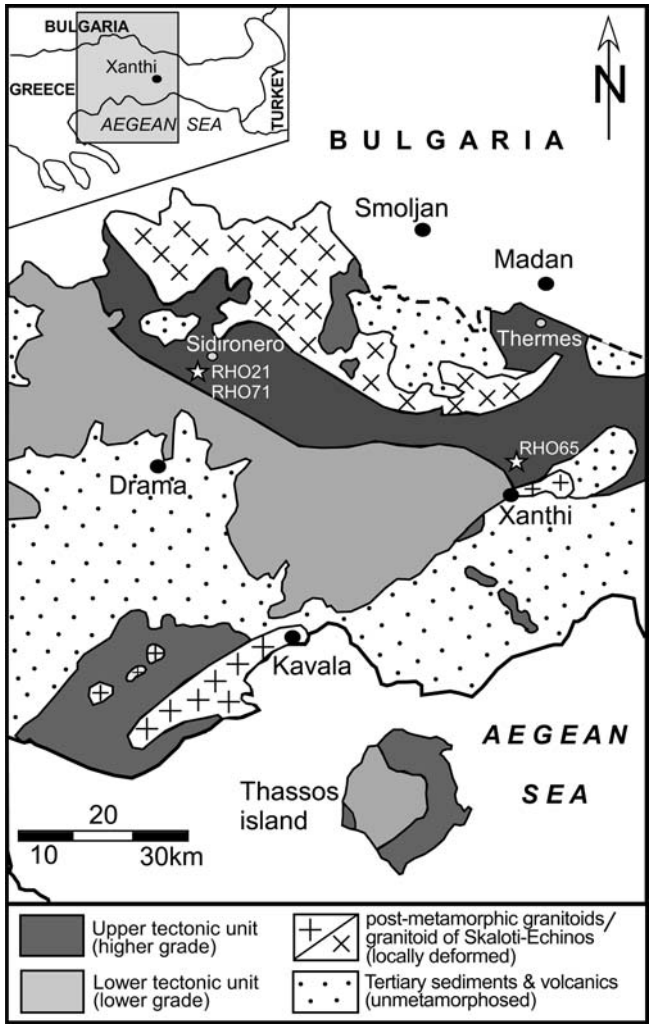

Fig. 2 Schematic map of West and Central Rhodope showing the main tectonic units (based on Mposkos 1989). The two locations of the samples dated in the present paper, north of Xanthi (sample RHO65) and north of Drama (samples RHO21 and RHO71) are marked by *asterisks*

minerals (hornblende, biotite, muscovite: 35–50 Ma) were interpreted as Eocene cooling ages of an amphibolite-facies metamorphism, while some much older dates, up to 95 Ma, reflect significant excess argon in the system (Liati 1986; Liati and Kreuzer 1990). Since in such high-pressure terranes only the youngest Ar-ages are closest to the time of metamorphism, a geologically meaningful metamorphic age would be closer to 35 Ma rather than 50 Ma. The 35 Ma dates refer probably to late stages of metamorphism (either to cooling or action of late fluids; e.g., Villa 1998). This is demonstrated by the 36.1 ± 1.2 Ma SHIMP-age of newly formed zircons in a late pegmatite (representing late metamorphic fluids) crosscutting the metamorphic rocks, close to Sminthi area (Liati and Gebauer 1999). Identical Ar–Ar (35.5 ± 0.4 Ma) and Rb–Sr (35.3 ± 0.4 Ma) biotite data, interpreted as cooling ages, are also known from orthogneisses of the Bulgarian Central Rhodope (Ovtcharova et al. 2003; Rohrmeier et al. 2002). U–Pb single monazite data from crosscutting non-deformed pegmatites in the Bulgarian Central Rhodope also yield 35.89 ± 0.20 Ma, in line with the above data (Ovtcharova et al. 2003).

In West Rhodope, K–Ar hornblende data from amphibolitized eclogites are scattering between ca. 45.5 and 50 Ma, while some much older dates reach ca. 81 Ma (Liati 1986). Similar to Central Rhodope, more or less significant excess argon is involved in the system, which makes these data relatively inconclusive. Nevertheless, the youngest dates (ca. 45.5 Ma) may be considered as closer to a geologically meaningful metamorphic age (see above).

Lips et al. (2000) report Ar–Ar laser probe mica data from rock samples dispersed over an E–W distance of more than ca. 220 km, extending from the west (Chalkidiki peninsula, i.e., Serbomacedonian massif sensu stricto) to the East Rhodope: for a quartz–feldspar mylonite and a calcite–quartz–feldspar mylonite in Chalkidiki peninsula, muscovite 'ages' of ca. 280 and 145 Ma are reported, while for a series of metamorphic rocks from the central and eastern Rhodope, white mica data ranging between ca. 42 and 15 Ma are given. The above authors interpret their data, as well as previously published geochronological data, as applying to the whole Rhodope (thereby mixing obviously different tectonic units) and suggest a continuous long-lasting kinematic system, operating for an unrealistically long time lasting between >100 and <15 Ma). A U–Pb monazite age of ca. 55 Ma, interpreted to reflect the time of the metamorphic peak, is reported for a migmatitic gneiss of Central Rhodope (Jones et al. 1994).

U–Pb ion microprobe zircon (SHRIMP) data in Central Rhodope (Thermes area) revealed an Eocene exhumation path lasting ca. 6 Ma (Liati and Gebauer 1999): ca. 42.2 ± 0.9 Ma for the time close to the pressure peak, 40.0 ± 1.0 Ma for the temperature peak (still at HP) and 36.1 ± 1.2 Ma for the late metamorphic stages. For East Rhodope, in the Kimi area, U–Pb SHRIMP-dating of magmatic and metamorphic zircon domains from a garnet-rich mafic rock gave an age of 117.4 ± 1.9 Ma, interpreted as the time of protolith crystallization, possibly of a HP cumulate, and an age of 73.5 ± 3.4, interpreted as the time of HP or UHP metamorphism (Liati et al. 2002; Liati et al. 2005a). The same authors report an age of 61.9 ± 1.9 Ma for the formation of a pegmatoid crosscutting the garnet-rich mafic rocks. This age is interpreted to mark the late stages of this metamorphic cycle. A similar Rb–Sr isochron age of 65.4 ± 0.7 Ma is reported by Mposkos and Wawrzenitz (1995) for muscovite and feldspar cores of an undeformed crosscutting pegmatite. The same authors report a Sm–Nd whole rock-garnet-cpx isochron age of a garnet pyroxenite from the same area at 119 ± 3.5 Ma, which they interpret as the age of HP metamorphism.

Regarding pre-metamorphic events, Hercynian ages are reported for magmatism, on the basis of conventional U–Pb dating of orthogneisses from Thassos island (U–Pb monazite: 285 ± 3 Ma; U–Pb zircon: ca. 260 Ma; Wawrzenitz 1997), from metagranitoids of the Bulgarian East Rhodope (310 ± 5.5 and 319 ± 9 Ma; Peytcheva and von Quadt 1995), as well from orthogneisses of Central Rhodope (294 ± 8 Ma; SHRIMP-ages by Liati and Gebauer 1999) and East Rhodope (313.9 ± 2.1 Ma; SHRIMP-ages by Liati and Fanning 2005). Finally, Jurassic crystallization (SHRIMP) ages of 151 ± 4 Ma are reported for a deformed biotite–metagranitoid rock in Central Rhodope, close to the village Oraion (Gebauer and Liati 1997).

Description of the samples dated

Three different rock types were collected and dated by SHRIMP analyses (see Figs. 2, 3 for sample locations). In both Central and West Rhodope, the rock types dated belong to the—generally defined—upper tectonic unit (see Overview and geological setting of the Rhodope section). In the following, only those petrographic and petrologic features of the rocks will be described, which are considered to be of importance for the interpretation of the geochronological data. Detailed petrology of the rocks is beyond the purpose of this paper.

Central Rhodope

Garnet–kyanite (grt–ky) paragneiss (sample RHO65)

This rock type was collected close to the road Xanthi-Echinos at the intersection to Stavroupolis (coordinates: N41°11.37.0; E24°51.66.7; Fig. 3). It is a strongly deformed, coarse-grained rock containing dispersed amphibolitized eclogite boudins. The common mineral assemblage is: garnet–kyanite–muscovite–biotite–plagioclase–quartz ± K-feldspar ± sillimanite ± staurolite. Accessory phases are rutile, ilmenite, zircon,

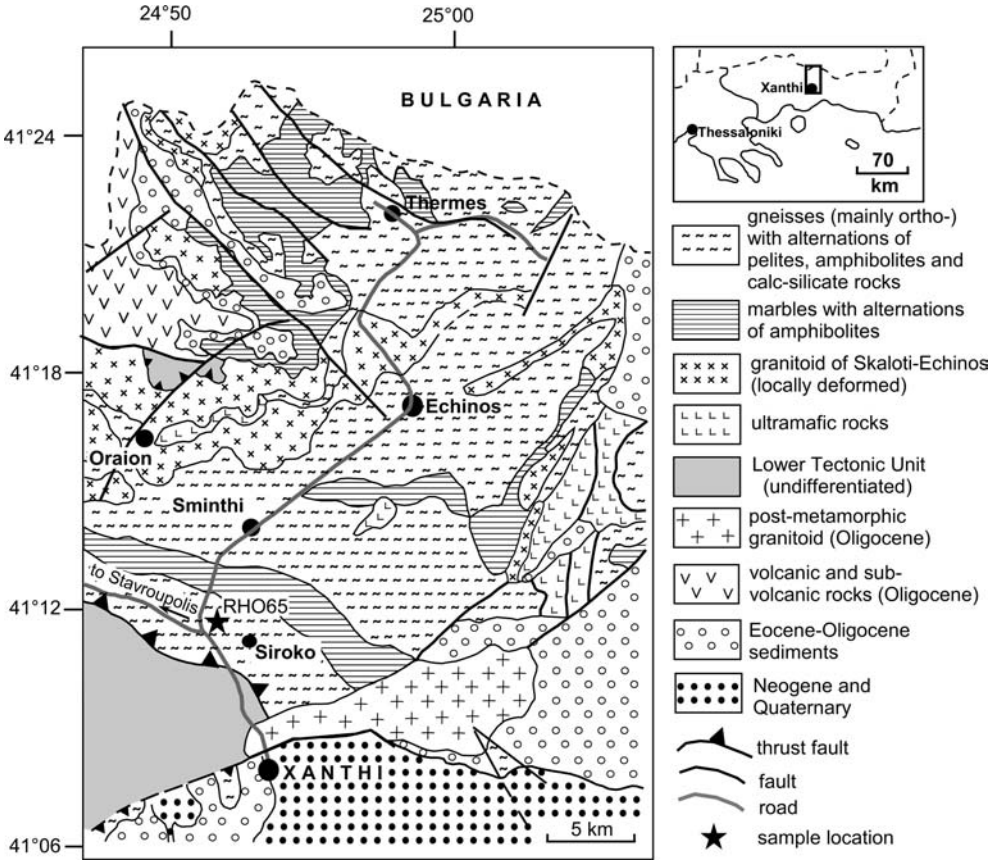

Fig. 3 Geological map of Central Rhodope, based on a provisional draft by S. Zachos and E. Dimadis (Institute of Geology and Mineral Exploration, Athens). The location of the garnet–kyanite (grt–ky) paragneiss (sample RHO65) is marked by a *asterisk*

apatite, sphene and tourmaline. *P-T* (equilibration) conditions of the last metamorphic overprint were ca. 8–9 kbar, 650–690°C (Liati 1986). However, the rock has probably been subjected to—at least—HP conditions of metamorphism: small biotite flakes or needles occur commonly at the grain boundaries of muscovite and/or in parallel intergrowth with muscovite and quartz and/or plagioclase (see also Mposkos and Liati 1993). These textural features are commonly reported from overprinted phengite-bearing HP rocks and are interpreted to indicate the pre-existence of high-Si phengite (compare e.g., Heinrich 1982; Franz et al. 1986; Nakamura 2003). Thus, this grt–ky paragneiss of Central Rhodope very likely underwent the same eclogite-facies metamorphism as the enclosed amphibolitized eclogite boudins (compare e.g., Liati 1986; Mposkos and Liati 1993). It is a common case in HP terranes (e.g., Adula nappe, Central Alps; Heinrich 1982) that meta-acidic and metapelitic rocks are more or less completely re-equilibrated during overprinting by a post-HP metamorphic stage and usually do not in fact preserve any relics of critical HP minerals. In contrast, for kinetic reasons, mafic rocks tend to preserve HP assemblages much better than non-mafic lithologies (e.g., Heinrich 1982; Koons and Thompson 1985). HP relics are best preserved in mafic lithologies also in the Rhodope zone (e.g., Liati 1986; Liati and Seidel 1996 and references therein).

Mposkos and Kostopoulos (2001) describe microdiamonds from the grt–ky paragneisses in our study area, thereby implying UHP conditions of metamorphism. Moreover, these authors interpret apatite inclusions and crystallographically oriented inclusions of quartz and rutile in garnet as exsolutions and therefore as an evidence of a preexisting majoritic garnet. Based on this interpretation they infer extreme UHP conditions of ca. 7 GPa, although the interpretation of these inclusions as exsolutions from a UHP majoritic garnet has since been questioned (see e.g., Beyssac and Chopin 2003). The least ambiguous evidence for UHP conditions in this area of Rhodope seems to be the presence of polycrystalline inclusions of quartz (former coesite) in garnet of amphibolitized eclogites, described by the same authors close to the grt–ky paragneisses (area of Pilima).

Because zircon is known to be an ideal host mineral to preserve (U)HP inclusions, numerous zircons from the grt–ky paragneiss studied here were examined with the Raman method, but neither coesite (or polycrystalline quartz) nor diamond were found as inclusions.

West Rhodope

Orthogneiss leucosome (sample RHO21)

An *orthogneiss leucosome* (sample RHO21), ca. 4–5 cm thick, was collected along the profile Drama-Sidironero,

9.5 km south of Sidironero (Fig. 2, coordinates N41°20.21.7; E24°12.33.1) as part of a migmatized orthogneiss (Fig. 4). Orthogneisses, partly migmatized, are abundant in West Rhodope. They constitute the lowermost lithologic formation, overlain by a series of alternating amphibolitized eclogites, marbles and rare micaschists and ultramafic rocks (see e.g., Mposkos et al. 1990; Chatzipanagis 1991; Mposkos 1994, for details). Pegmatites often crosscut all above rock types.

The common mineral assemblage of the migmatized orthogneiss (palaeosome) is: K-feldspar–plagioclase–quartz–biotite–muscovite ± garnet ± clinozoisite/zoisite. Metamorphic conditions are of the upper amphibolite-facies; critical HP minerals are lacking in this rock type (see also Mposkos et al. 1990).

Amphibolitized eclogite (sample RHO71)

An *amphibolitized eclogite* (sample RHO71, same coordinates as RHO21), pervasively overprinted under upper amphibolite-facies metamorphism was collected at the immediate contact to above migmatized orthogneiss. The common mineral assemblage of this rock is: garnet–hornblende–plagioclase–quartz–clinozoisite–epidote ± sodic augite/albite symplectites ± diopside ± biotite ± chlorite–rutile–titanite. Symplectites of hornblende–plagioclase were observed around garnet (kelyphites). The presence of sodic augite/albite symplectites indicates the pre-existence of omphacite. Hornblende + plagioclase kelyphites around garnet are also a known feature in overprinted eclogites and form by a reaction of omphacite + garnet. For details on textural features, especially symplectites, in retrograded eclogites, the reader is referred to e.g., Heinrich (1986) or Yang et al. (2004) and references therein. Rutile is almost always surrounded by titanite. As a rule, rutile is the HP Ti-phase in rocks of basic composition (e.g., Hellman and Green 1979; Xiong et al. 2005). Peak *P-T* conditions of the eclogite stage cannot be obtained for these amphibolitized eclogites, because the original high-*P* paragenesis has been destroyed, due to strong overprint. Based on the maximum jadeite content (19 mol%; Mposkos et al. 1990) preserved in the sodic augite (breakdown product of omphacite), pressures of ca. 11 kbar (for $T = 650°C$) are inferred as minimum *P* conditions along the exhumation path of the amphibolitized eclogites in West Rhodope.

Analytical techniques and data evaluation

U–Pb dating of zircon

The major part of the data listed in the present paper were obtained on SHRIMP II at the Geological Survey of Canada in Ottawa. Analyses number 37 to 55 of Table 1 were obtained on SHRIMP II at the Research School of Earth Sciences, The Australian National University (ANU), Canberra. A spot size of about 25 μm was used. In a few cases (very narrow zircon domains), the spot size used was ca. 10 μm. For data collection, seven scans through the critical mass range were made. For a detailed description on the SHRIMP technique, data processing including the reasons for using mainly $^{206}Pb/^{238}U$-ages for Phanerozoic zircons, the reader is referred to Compston et al. (1992), Williams (1998) or Stern (1997).

Fig. 4 Photograph showing the migmatized orthogneiss of West Rhodope, of which a leucosome (sample RHO21, see Fig. 2) was dated in this study

Cathodoluminescence (CL)

SHRIMP-dating was assisted by CL imaging of the zircon crystals. CL images allow a differentiation of the individual zircon crystals into various domains. This technique provides valuable information on the formation history of the different sectioned zircon domains and, most importantly, helps to avoid analyzing more than one domain at a time and obtain mixed ages.

All CL pictures were photographed from a split screen on a CamScan CS 4 scanning electron microscope (SEM) at ETH in Zurich operating at 13 kV. The same sample mount was used later for both the CL studies and SHRIMP-dating. The SEM is equipped with an ellipsoidal mirror that is located close to the sample and amplifies the CL-signal (see Gebauer 1996 for detailed technical description). In general, strong CL in the zircon (brighter appearance) reflects low amounts of minor and trace elements, weak CL (darker appearance) indicates high amounts of minor and trace elements, including U (e.g., Sommerauer 1974). Thus, the U-contents can be qualitatively predicted via CL.

Data evaluation

For the calculation of the $^{238}U/^{206}Pb$ ratios and ages, the data were corrected for common Pb using the ^{207}Pb correction method, following the standard procedures of Compston et al. (1992) and Williams et al. (1996). For the inherited zircons (Proterozoic and older) the ages are given as ^{204}Pb-corrected, $^{206}Pb/^{238}U$-ages for analytically concordant data and as ^{204}Pb-corrected, $^{207}Pb/^{206}Pb$-ages for analytically discordant data (the latter applies only for analysis 8 of Table 1). It is reminded that the $^{207}Pb/^{206}Pb$-ages are minimum ages for the magmatic formation of these domains.

The data obtained here are graphically presented on Tera–Wasserburg (TW) diagrams (Tera and Wasserburg 1972), where total $^{207}Pb/^{206}Pb$ versus the calibrated, total $^{238}U/^{206}Pb$ is plotted. This diagram allows fast estimation of the amount of common Pb of the projected analyses. The amount of common Pb was calculated using the isotope composition at the time of zircon formation obtained from the model of Cumming and Richards (1975). It is noted that our results were the same, irrespective of the common Pb correction (e.g., composition of the gold coating or the surface common Pb), because of the low amount of common Pb of our samples (analyses are plotted close to the concordia curve on the TW diagrams). The ellipses on the TW diagrams are plotted with a 2σ error. For the individual analyses listed in Table 1 and shown on the zircon CL-images, 1σ errors are given. Finally, the ages were calculated from the lower intercept of the regression line with the Concordia in the TW diagrams. The error on the ages is at the 95% confidence level (cl). It is noted that the intercept ages are completely in agreement with the calculated weighted mean ages. For all diagrams and age calculations, the ISOPLOT program of Ludwig (2000) was used.

REE analyses of zircon

REE analyses were obtained by LA-ICPMS (Excimer 193-nm ArF Laser, coupled with an ELAN6100 quadrupole MS) at the Institute of Isotope Geology and Mineral Resources, ETH Zurich (sample RHO71 and RHO1 in Table 2) and by SHRIMP II at the Research School of Earth Sciences, ANU, Canberra (sample RHO65 in Table 2). For the LA-ICPMS analyses, the SRM 610 glass from NIST was used as an external

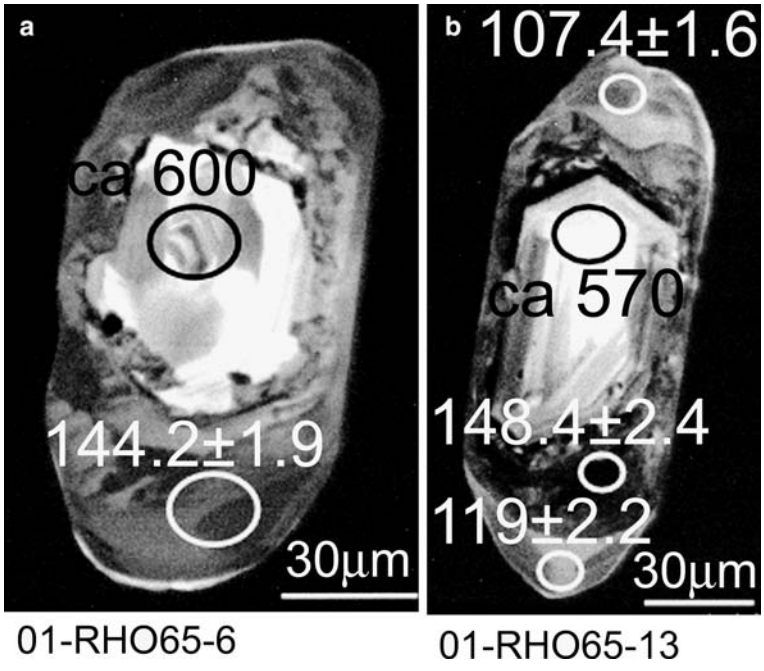

Fig. 5 Cathodoluminescence images of zircons from the grt–ky paragneiss of Central Rhodope. Zircon crystals consist of detrital cores surrounded by metamorphic rims (*gray in CL*). In crystal **b**, two metamorphic rims are recognized: a darker inner rim and a brighter outermost one. The *outermost rims* show various amounts of Pb-loss, due to the influence of post-ca. 149 Ma metamorphic event(s) (see text for details). *Circles* correspond to SHRIMP-spots. The ages shown are $^{206}Pb/^{238}U$ ages and the errors are 1σ

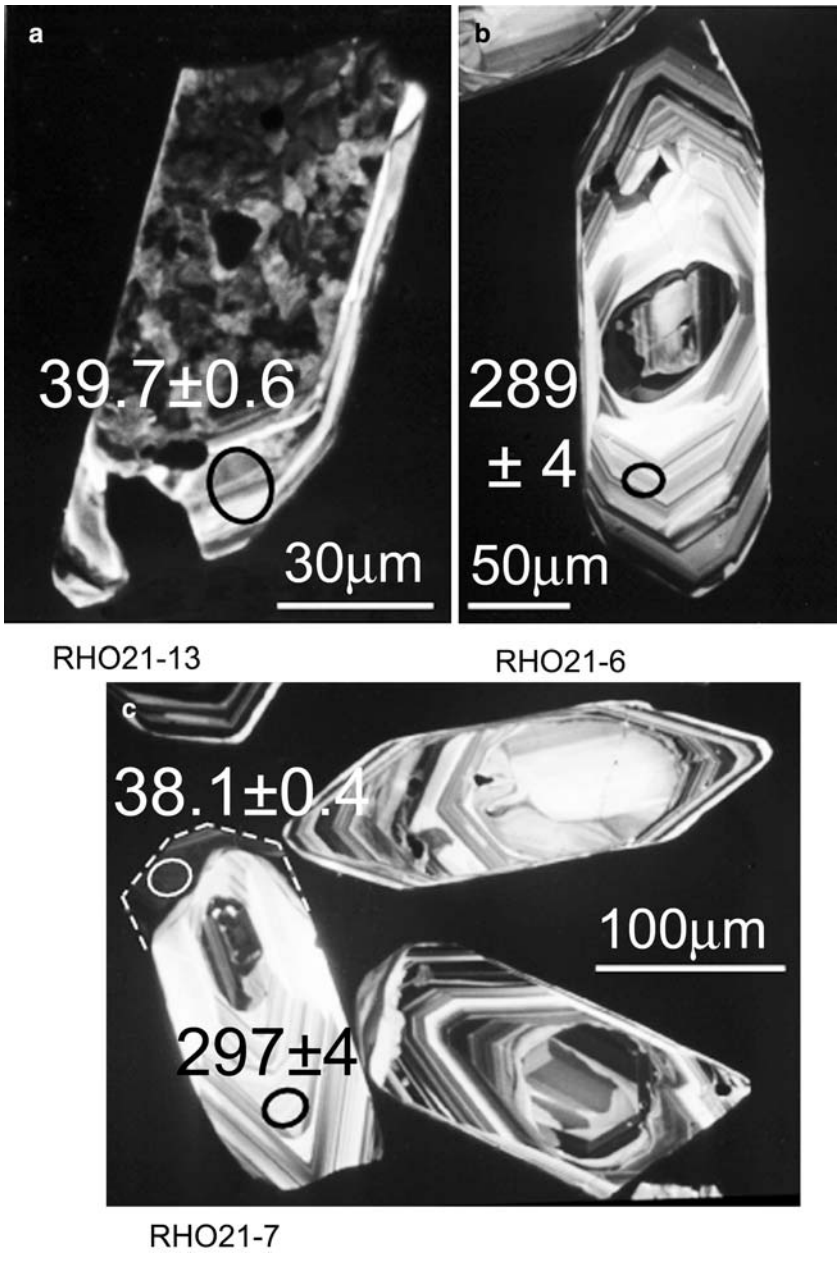

Fig. 6 Cathodoluminescence images of zircon crystals from the migmatite leucosome of West Rhodope. The zircons consist largely of a Hercynian oscillatory zoned part, which precipitated during crystallization of the granitoid protolith. Older inherited cores are sometimes present in the Hercynian zircon domains (e.g., crystal **b** and lower right crystal of **c**). In **a** and leftmost crystal of **c**, an oscillatory rim surrounds the magmatic core (best visible in **a**). This outer oscillatory rim is ca. 39 Ma old, and its formation is genetically related to migmatization and leucosome formation. The *white dashed line* on the leftmost crystal of **c** is drawn to better mark the outline of the crystal. *Circles* correspond to SHRIMP-spots. The ages shown are $^{206}Pb/^{238}U$ ages and the errors are 1σ

standard. Repetition rate was 10 Hz and the sizes of the spots were 30, 40 and 60 μm in diameter, depending on the size of the zircon domains. Oxide production rate was tuned to $<0.5\%$ ThO. A detailed compilation of instrument and data acquisition parameters for the LA-ICPMS is given in Pettke et al. (2004). The SHRIMP REE analyses were carried out using SHRIMP II in energy filtering mode following procedures similar to those described in Hoskin (1998) and Hoskin and Ireland (2000). The NIST glass was used to set up the REE peaks monitor interferences, and to derive the sensitivity factors used to calculate the REE concentrations (Hoskin 1998). During the course of the analytical session, chips of the 91,500 reference zircon were analyzed in conjunction with the unknowns. The size of the spots was ca. 30 μm in diameter.

Morphological characteristics and CL-imaging of zircon

Central Rhodope

Garnet–kyanite paragneiss (sample no. RHO65)

Zircons obtained from this rock are elongate with rounded outlines. They are relatively large, ranging between 120–220 μm in length and 60–120 μm in width. CL-images of these zircons show that they consist of a detrital core, surrounded by a wide (sometimes up to 60 μm broad) metamorphic domain (Fig. 5). The detrital cores usually show oscillatory zoning, inherited from their igneous protolith. The metamorphic rims are relatively homogeneous in CL, while some of them show

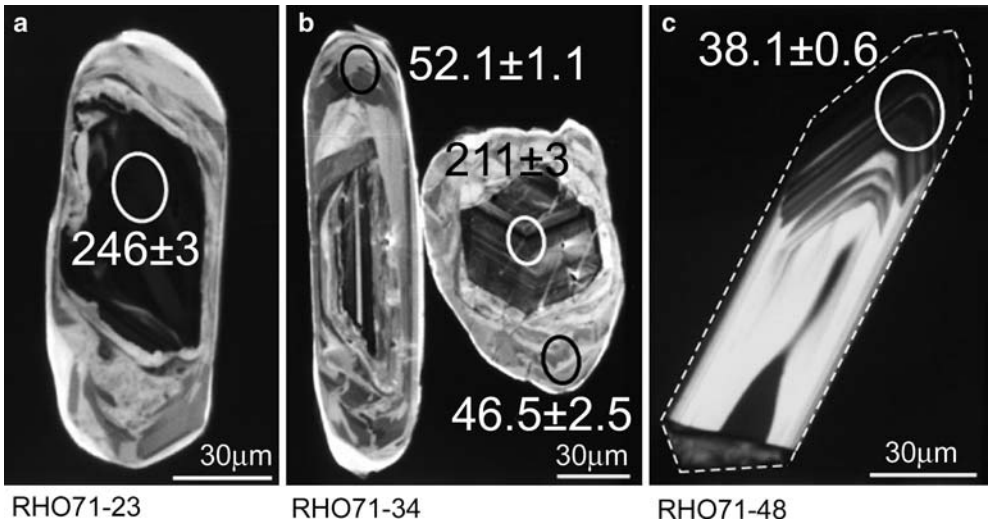

Fig. 7 Cathodoluminescence images of zircon crystals from the amphibolitized eclogite of West Rhodope. Zircons **a** and **b** consist of a co-magmatic core with more or less pronounced oscillatory zoning and a broad metamorphic rim. The cores crystallized at 245.6 ± 3.9 Ma in the gabbroic protolith of the eclogites. Note the fractures crosscutting the oscillatory cores (**b**). SHRIMP analyses on such fractures show Pb-loss (e.g., **b**). In contrast, SHRIMP spot in **a** is located on a fracture-free core. The rims formed during HP metamorphism at 51 ± 1 Ma. Note the presence of a CL-bright, very thin distinct rim at the outermost part of zircons **a** and **b**, which indicates incipient recrystallization, probably due to the influence of a post-51 Ma metamorphic/fluid event. Zircon **c** with completely different CL characteristics shows pronounced oscillatory zoning and has sharp edges. The *white dashed line* is drawn to better mark the outline of this crystal (see text for interpretation). *Circles* correspond to SHRIMP-spots. The ages shown are $^{206}Pb/^{238}U$ ages and the errors are 1σ

sector zoning. In some cases, two distinct metamorphic rims, an inner and an outer one, are observed around the detrital cores (e.g., Fig. 5b). As shown below, these two distinct rim domains yield different ages.

West Rhodope

Orthogneiss leucosome (sample no. RHO21)

Zircons obtained from this rock are commonly ca. 200–250 μm long prismatic crystals, usually consisting of a single domain with strong oscillatory zoning, typical for melt- (or fluid-) precipitated zircons (Fig. 6b, c). Sometimes, inherited cores are present within these large oscillatory zoned crystals (e.g., Fig. 6b). An outermost rim domain with a more or less clearly expressed oscillatory zoning is observed around the core of a few crystals (Fig. 6a and leftmost crystal of c). In view of the SHRIMP-results (see below), formation of this outermost rim is interpreted to be genetically related to leucosome formation during migmatization.

Amphibolitized eclogite (sample no. RHO71)

In this sample, zircons occur as ca. 200–250 μm long prismatic crystals, usually with rounded edges. The relatively large size of the zircon crystals suggests that the protolith of this amphibolitized eclogite was a gabbro rather than basalt, because such large co-magmatic zircons cannot grow from the rapidly cooling basaltic melts. Zircon crystals display an oscillatory zoned (magmatic) core and a relatively broad metamorphic rim (e.g., Fig. 7a, b). The broad metamorphic rims probably resulted from a strong recrystallization of the originally magmatic (gabbroic) zircons during metamorphism. Ghost oscillatory zoning, left over from the magmatic zircon, is still observed in some metamorphic zircon rims (Fig. 7a). A very thin rim, very bright in CL, occurs at the outermost part of the zircon crystals (Fig. 7a, b). This thin outermost rim is probably genetically related to a late metamorphic overpint. The magmatic zircon cores are often crosscut by numerous cracks (e.g., cores of Fig. 7b). These cracks acted probably as channels for fluids, which leached trace elements, as well as radiogenic Pb from the original magmatic cores (see below, under SHRIMP results section). Interestingly, among the many mounted zircon crystals of this eclogite (ca. 60), one crystal shows a completely different shape and CL pattern: it is euhedral, with sharp edges and consists of only one domain with strong oscillatory zoning (Fig. 7c). The possible provenance and significance of this zircon crystal is discussed below (SHRIMP results section), together with the SHRIMP-results.

SHRIMP results

Central Rhodope

Garnet–kyanite paragneiss (no. RHO65)

Detrital zircon cores Thirty-one analyses have been carried out on detrital zircon cores of this rock. Out of

Table 1 U, Th, Pb SHRIMP data for detrital, co-magmatic, metamorphic and inherited zircon domains from different metamorphic rock types of the Rhodope zone, Northern Greece

	Sample	U (ppm)	Th (ppm)	Th/U	Rad. Pb (ppm)	f_{206}	$^{238}U/^{206}Pb$ (uncorrected)	± error (1σ)	$^{207}Pb/^{206}Pb$ (uncorrected)	± error (1σ)	Age (Ma) $^{206}Pb/^{238}U$	± error (1σ)
Central Rhodope												
Garnet–kyanite paragneiss (RHO65)												
Detrital zircon cores												
1.	00-RHO65-1d	165	108	0.65	134	< 0.01	0.265	0.001	1.5345	0.0267	3,234	45
2.	01-RHO65-1.3	54	37	0.69	40	0.16	1.650	0.028	0.2248	0.0020	3,052	42
3.	01-RHO65-1.2	119	69	0.58	81	< 0.01	1.774	0.028	0.2273	0.0010	2,882	36
4.	01-RHO65-2.3	111	18	0.16	59	< 0.01	1.985	0.035	0.1816	0.0038	2,628	38
5.	01-RHO65-8.1	50	118	2.38	27	0.39	2.974	0.041	0.1178	0.0009	1,863	23
6.	00-RHO65-13.1	60	47	0.79	23	< 0.01	0.126	0.001	3.0041	0.1077	1,852	58
7.	00-RHO65-5.1	52	34	0.65	19	< 0.01	0.118	0.001	3.0164	0.0636	1,844	34
8.	01-RHO65-7.2	133	47	0.35	43	< 0.01	3.297	0.049	0.1300	0.0009	2,097	13
9.	00-RHO65-7.2	781	275	0.35	250	< 0.01	0.115	0.000	3.3274	0.0907	1,640	41
10.	00-RHO65-6.1	77	55	0.71	9	< 0.01	0.060	0.001	9.0724	0.3273	674	23
11.	00-RHO65-10.1	472	455	0.96	59	< 0.01	0.062	0.001	9.5200	0.1928	644	12
12.	01-RHO65-12.1	75	104	1.39	10	0.21	9.999	0.154	0.0616	0.0006	613	10
13.	00-RHO65-1.C	143	47	0.33	14	0.12	0.062	0.000	10.442	0.2248	589	12
14.	01-RHO65-10.1	178	119	0.67	18	0.18	10.66	0.175	0.0606	0.0005	577	9
15.	00-RHO65-2.1	122	222	1.83	16	0.36	0.060	0.002	10.756	0.2057	571	11
16.	00-RHO65-3.1	437	187	0.43	41	< 0.01	0.060	0.001	10.917	0.2133	557	8
17.	01-RHO65-3.1	682	85	0.13	58	< 0.01	11.09	0.162	0.0613	0.0005	565	11
Metamorphic zircon rims												
18.	00-RHO65-4.2	822	2	0.003	18	0.39	40.99	0.81	0.0483	0.0008	155.6	3.1
19.	00-RHO65-10.2	1,110	2	0.002	24	< 0.01	41.23	0.75	0.0496	0.0004	154.4	2.8
20.	01-RHO65-14.1	1,748	3	0.002	38	0.08	41.90	0.62	0.0495	0.0004	152.0	2.2
21.	01-RHO65-2.1	908	2	0.002	19	0.17	42.13	0.58	0.0498	0.0004	151.1	2.1
22.	00-RHO65-12.2	966	3	0.003	20	0.12	42.54	0.83	0.0490	0.0004	149.8	2.9
23.	01-RHO65-13.4	2527	3	0.001	53	< 0.01	42.89	0.71	0.0502	0.0004	148.4	2.4
24.	01-RHO65-2.2	994	2	0.002	21	0.18	43.42	0.60	0.0504	0.0005	146.5	2.0
25.	01-RHO65-12.2	1123	2	0.001	23	0.23	43.49	0.64	0.0503	0.0004	146.3	2.1
26.	00-RHO65-1.B	1,008	3	0.004	21	0.12	43.50	0.74	0.0501	0.0002	146.3	2.5
27.	00-RHO65-7.1	724	2	0.002	15	0.02	43.86	0.83	0.0482	0.0007	145.5	2.7
28.	00-RHO65-1.A	1,039	3	0.003	22	0.15	43.66	0.77	0.0519	0.0004	145.5	2.5
29.	00-RHO65-5.2	1,140	7	0.006	23	< 0.01	43.94	0.84	0.0502	0.0002	144.9	2.7
30.	*01-RHO65-6.1*	*1,159*	*5*	*0.005*	*24*	*0.16*	*44.15*	*0.59*	*0.0501*	*0.0003*	*144.2*	*1.9*
31.	*01-RHO65-7.1*	*1,053*	*3*	*0.003*	*21*	*0.02*	*5.06*	*0.61*	*0.0493*	*0.0003*	*141.4*	*1.9*
32.	*01-RHO65-1.1*	*481*	*1*	*0.003*	*9*	*0.86*	*48.12*	*0.68*	*0.0536*	*0.0008*	*131.8*	*1.8*
33.	*01-RHO65-10.2*	*455*	*1*	*0.003*	*8*	*0.30*	*49.27*	*0.78*	*0.0510*	*0.0006*	*129.1*	*2.0*
34.	*01-RHO65-13.2*	*538*	*1*	*0.003*	*9*	*0.10*	*53.10*	*0.98*	*0.0569*	*0.0012*	*119.0*	*2.2*
35.	*01-RHO65-13.3*	*683*	*2*	*0.004*	*11*	*0.27*	*59.08*	*0.89*	*0.0543*	*0.0004*	*107.4*	*1.6*
36.	*01-RHO65-10.3*	*426*	*1*	*0.002*	*5*	*0.35*	*75.58*	*1.20*	*0.0657*	*0.0009*	*82.8*	*1.3*
											LI: 148.8 ± 2.2 Ma	
West Rhodope												
Migmatite leucosome (RHO21)												
Co-magmatic zircon domains												
37.	RHO21-6.1	171	118	0.69	7	0.35	21.71	0.27	0.0549	0.0016	289.4	3.7
38.	RHO21-7.2	186	166	0.89	8	0.43	21.11	0.25	0.0557	0.0018	297.0	3.5
39.	RHO21-16.1	410	165	0.40	16	0.10	21.61	0.24	0.0529	0.0007	291.3	3.3
40.	RHO21-16.2	576	328	0.57	24	1.29	20.88	0.16	0.0627	0.0012	297.7	2.4
41.	RHO21-18.2	1,220	148	0.12	49	0.06	21.41	0.14	0.0527	0.0006	294.1	1.9
42.	RHO21-18.3	541	15	0.03	22	0.11	21.01	0.17	0.0532	0.0014	299.5	2.5
43.	RHO21-22.2	880	57	0.07	36	0.07	21.20	0.20	0.0528	0.0008	296.9	2.8
44.	RHO21-8.1	971	62	0.06	39	0.15	21.43	0.15	0.0534	0.0010	293.5	2.1
45.	RHO21-21.1	505	284	0.56	20	0.13	21.62	0.18	0.0531	0.0010	291.1	2.4
46.	RHO21-21.2	533	596	1.12	21	0.27	21.79	0.25	0.0542	0.0012	288.5	3.4
47.	RHO21-22.1	59	44	0.74	2	< 0.01	21.97	0.37	0.0512	0.0017	287.2	4.7
48.	*RHO21-7.1*	*202*	*164*	*0.81*	*8*	*0.12*	*22.69*	*0.30*	*0.0528*	*0.0012*	*277.7*	*3.7*
											LI: 294.3 ± 2.4 Ma	
Inherited zircon core domains												
49.	RHO21-27.1	122	63	0.51	10	0.03	10.38	0.13	0.0600	0.0009	593.0	7.0
50.	RHO21-27.3	149	93	0.63	12	0.66	10.61	0.12	0.0647	0.0015	574.0	7.0
51.	RHO21-28.3	740	610	0.82	61	0.11	10.39	0.10	0.0605	0.0006	591.8	5.7
52.	RHO21-18.1	527	247	0.47	43	< 0.01	10.56	0.11	0.0591	0.0005	583.5	6.1

Table 1 (Contd.)

	Sample	U (ppm)	Th (ppm)	Th/U	Rad. Pb (ppm)	f_{206}	$^{238}U/^{206}Pb$ (uncorrected)	± error (1σ)	$^{207}Pb/^{206}Pb$ (uncorrected)	± error (1σ)	Age (Ma) $^{206}Pb/^{238}U$	± error (1σ)
	Metamorphic zircon rims											
53.	RHO21-13.1	1,328	4	0.003	7	1.41	159.56	2.54	0.0580	0.0018	39.7	0.6
54.	RHO21-7.3	998	1	0.001	5	1.09	166.93	1.80	0.0554	0.0021	38.1	0.4
55.	*RHO21-11.1*	*789*	*1*	*0.001*	*4*	*0.29*	*154.62*	*1.96*	*0.0492*	*0.0014*	*41.4*	*0.5*
	Amphibolitized eclogite (RHO71)											
	Co-magmatic zircon domains (cores)											
56.	RHO71-16.1	547	195	0.36	21	0.01	25.42	0.36	0.0579	0.0007	246.7	3.4
57.	RHO71-23.1	882	352	0.40	35	< 0.01	25.68	0.36	0.0529	0.0009	245.7	3.4
58.	RHO71-16.2	272	61	0.22	10	0.01	25.58	0.38	0.0609	0.0009	244.3	3.6
59.	*RHO71-16.3*	*317*	*93*	*0.29*	*11*	*0.06*	*25.33*	*0.40*	*0.0972*	*0.0017*	*235.5*	*3.7*
60.	*RHO71-13.1*	*433*	*324*	*0.75*	*18*	*0.02*	*26.84*	*0.39*	*0.0658*	*0.0020*	*231.5*	*3.3*
61.	*RHO71-45.2*	*289*	*164*	*0.57*	*11*	*0.01*	*28.60*	*0.43*	*0.0596*	*0.0011*	*219.1*	*3.2*
62.	*RHO71-34.1*	*493*	*199*	*0.40*	*17*	*0.01*	*29.94*	*0.47*	*0.0552*	*0.0018*	*210.5*	*3.3*
63.	*RHO71-38.1*	*463*	*401*	*0.87*	*18*	*0.02*	*30.01*	*0.54*	*0.0642*	*0.0014*	*207.7*	*3.7*
64.	*RHO71-5.1*	*391*	*153*	*0.39*	*12*	*0.01*	*33.22*	*0.84*	*0.0611*	*0.0014*	*188.6*	*4.7*
											LI: 245.6 ± 3.9 Ma	
	Inherited core											
65.	RHO71-14.1	171	104	0.63	12	0.01	14.46	0.22	0.0649	0.0015	430.0	7.0
	Metamorphic zircon rims											
66.	RHO71-41.1	80	0	0.005	1	0.12	108.66	2.64	0.1440	0.0113	51.8	1.5
67.	RHO71-43.1	169	1	0.005	1	0.09	115.02	2.17	0.1177	0.0059	50.8	1.0
68.	RHO71-43.2	130	0	0.004	1	0.12	112.72	2.88	0.1395	0.0067	50.3	1.4
69.	RHO71-11.3	231	1	0.004	2	0.19	102.35	2.07	0.1947	0.0054	51.0	1.1
70.	RHO71-34.3	162	1	0.004	1	0.07	114.27	2.35	0.1042	0.0038	52.1	1.1
71.	RHO71-34.2	101	1	0.01	1	0.13	119.97	6.23	0.1503	0.0099	46.5	2.5
72.	*RHO71-48.1*	*835*	*906*	*1.08*	*6*	*0.01*	*166.19*	*2.54*	*0.0585*	*0.0014*	*38.1*	*0.6*
											LI: 51.0 ± 1.0 Ma	

Notes: f_{206} denotes the percentage of ^{206}Pb that is common Pb. *LI* lower intercept
Analyses 37–55 were obtained at The ANU, Canberra, all others at GSC, Ottawa
Analyses in italics were not considered for the age calculation (see text for details)
Proterozoic (and older) ages are given as ^{204}Pb-corrected, $^{206}Pb/^{238}U$-ages for analytically concordant data; for the analytically discordant data of analysis 8, the ^{204}Pb-corrected, $^{207}Pb/^{206}Pb$-age is given (see Data evaluation section)

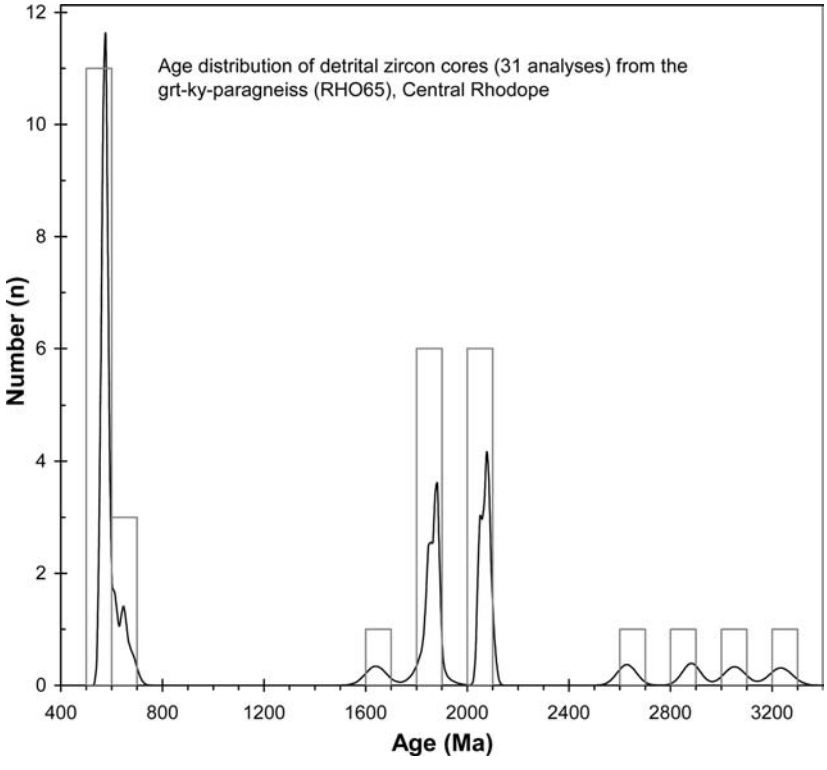

Fig. 8 Cumulative probability distribution and histogram showing the age distribution of inherited zircon cores from the grt–ky paragneiss of Central Rhodope (RHO65). Prevailing age concentrations are observed in the range 500–700 Ma and around 2 Ga (see text)

these analyses, 17 have been run to completion and are listed in Table 1, whereas 14 analyses have been aborted after the first two scans and gave only a rough estimate of the time of formation. A complete provenance study of detrital zircon ages with a high statistical degree of certainty is beyond the purpose of the present paper. The results given below are considered as sufficiently informative for the maximum age of sedimentation. Of the 14 analyses, which were not run to completion, 6 yielded dates between 600–500 Ma, 5 between 2 and 2.1 Ga and 3 between 1.8 and 1.9 Ga. In the histogram of Fig. 8, the distribution of the 31 ages of detrital cores is shown. The prevailing concentration of ages between 500 and 700 Ma, and between 2 and 2.1 Ga is typical for a Gondwana provenance (e.g., Gebauer 1993; Nance and Thompson 1996; Valverde-Vaquero et al. 2000 and references therein). The oldest age obtained was 3,234 ± 45 Ma. The youngest detrital core yielded an Upper Proterozoic age of ca. 560 Ma (analysis 16 of Table 1), which is considered as a maximum age for the sedimentation. The degree of concordance of the detrital cores ranges between 86 and 103%. No Hercynian age has been obtained from the detrital cores of this rock, which indicates that its sedimentation was possibly completed before erosion of Hercynian rocks.

Metamorphic zircon rims Nineteen analyses were obtained from the metamorphic rims. On a Tera–Wasserburg diagram (Fig. 9; see also Data evaluation section), 12 analyses define a mixing line between a common Pb and a radiogenic $^{238}U/^{206}Pb$ end member intersecting the Concordia at 148.8 ± 2.2 Ma (MSWD: 2.0). This age is interpreted as the time close to HP [or UHP] metamorphism (see details below, Limitations of the metamorphic SHRIMP-ages and Geological implications sections).

Seven spots yielded younger dates, down to ca. 83 Ma, thus indicating Pb-loss during subsequent metamorphic/fluid event(s), at least younger than the youngest 'age' obtained from the metamorphic outermost rims (82.8 ± 1.3 Ma). A variable Pb-loss of the outermost zircon rims is graphically illustrated on a normal (Wetherill) Concordia diagram (^{208}Pb-corrected data; Fig. 10). All analyses with various amounts of Pb-loss are aligned along the Concordia line. It is worth mentioning that for the zircon crystals, which show two distinct metamorphic rims in CL (see above, under Central Rhodope section and Fig. 5b), the inner rim was always dated at ca. 148 Ma within uncertainty, while the outer rim always yielded significantly younger discordant dates reflecting variable Pb-loss. Previous K–Ar muscovite data from the same rock type at 35.3 ± 0.3 Ma (Liati 1986; Liati and Kreuzer 1990) independently indicate the influence of a younger, Upper Eocene event (see below, Metamorphism section).

West Rhodope

Orthogneiss leucosome (no. RHO21)

Nineteen spots in zircons from the leucosome were analyzed: 16 from the large oscillatory zoned crystals (or core domains) and three from the oscillatory zoned rims. On a Tera–Wasserburg diagram (Fig. 11), 11 analyses of the oscillatory zoned crystals (cores) define a mixing line between common Pb and a radiogenic $^{238}U/^{206}Pb$ end

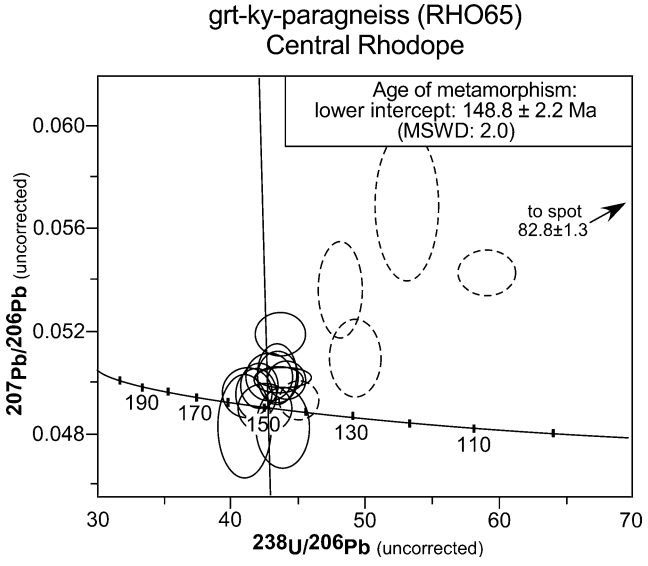

Fig. 9 Tera–Wasserburg diagram with data of zircons from the grt–ky paragneiss of Central Rhodope. Twelve analyses from the metamorphic zircon rims plot on a mixing line with common Pb and radiogenic $^{238}U/^{206}Pb$ as end members, and yield a lower intercept $^{206}Pb/^{238}U$ age of 148.8 ± 2.2 Ma. Six analyses plot to the right side of the mixing line (*dashed ellipses*), due to Pb-loss (see text)

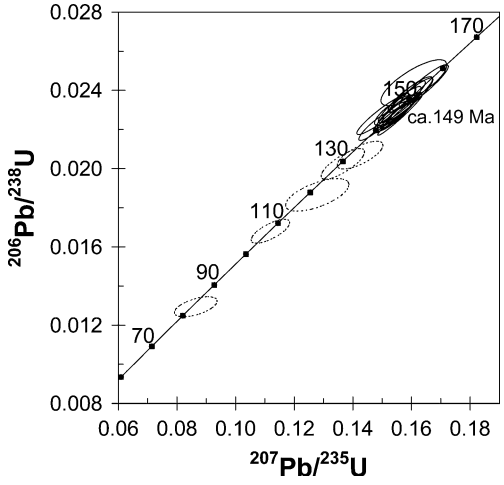

Fig. 10 Wetherill concordia diagram (based on ^{208}Pb-corrected data) of metamorphic zircon domains from the grt–ky paragneiss (RHO65) showing various amounts of Pb-loss after ca. 149 Ma (*dashed ellipses aligned along the Concordia*). All data plotted below the ca. 149 Ma cluster are from the outermost zircon rims (e.g., Fig. 5b). Variable Pb-loss is probably connected to a younger metamorphic overprint (see text)

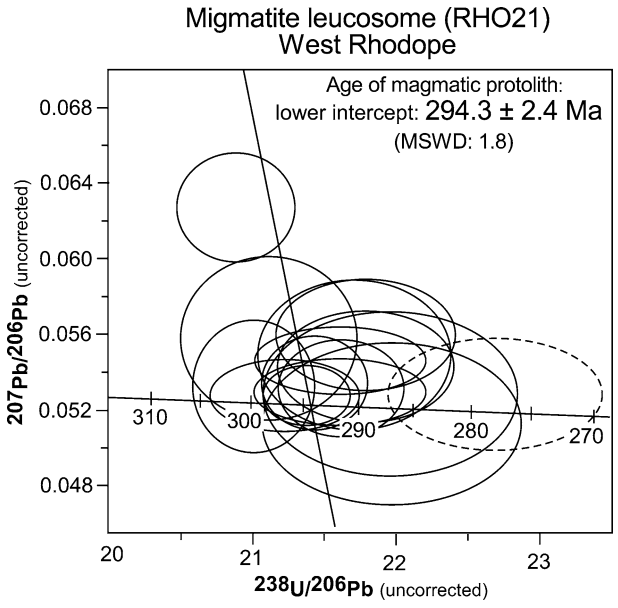

Fig. 11 Tera–Wasserburg diagram with data of zircons from the migmatite leucosome of West Rhodope (RHO21). Eleven analyses from the co-magmatic large oscillatory zoned zircon domains plot on a mixing line with common Pb and radiogenic $^{238}U/^{206}Pb$ as end members, intersecting the Concordia at a $^{206}Pb/^{238}U$ age of 294.3 ± 2.4 Ma, which is interpreted as the time of crystallization of the magmatic (granitoid) protolith of the orthogneiss. One analysis plots to the right side of the mixing line (*dashed ellipse*), because of Pb-loss, due to later metamorphism (see text)

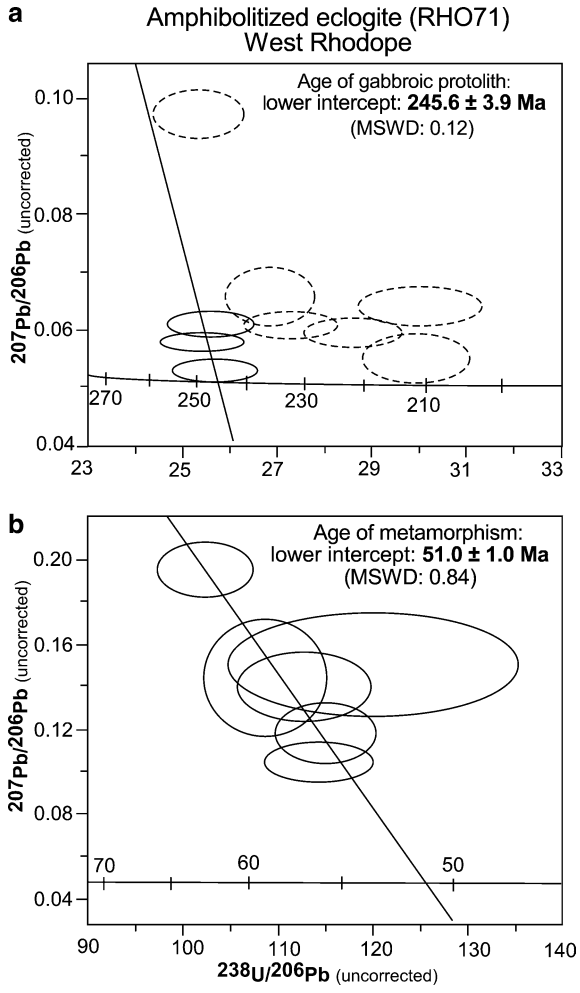

Fig. 12 Tera–Wasserburg diagrams with data of zircons from the amphibolitized eclogite of West Rhodope (RHO71). In **a**, three analyses from the oscillatory zoned zircon cores, free of fractures, plot on a mixing line with common Pb and radiogenic $^{238}U/^{206}Pb$ as end members intersecting the Concordia at a $^{206}Pb/^{238}U$ age of 245.6 ± 3.9 Ma, which is interpreted as the time of crystallization of the magmatic (gabbroic) protolith. Six analyses plot to the right side of the mixing line (*dashed ellipses*). These analyses show various amounts of Pb-loss, because the SHRIMP spots were partly located on crosscutting fractures. Such fractures facilitate fluid circulation and leaching of radiogenic Pb during metamorphic events (see text). In **b**, six analyses from the metamorphic rims plot on a mixing line with common Pb and radiogenic $^{238}U/^{206}Pb$ as end members intersecting the Concordia at a $^{206}Pb/^{238}U$ age of 51.0 ± 1.0 Ma, which is interpreted as the time of HP metamorphism (see text)

member intersecting the Concordia at a $^{206}Pb/^{238}U$ age of 294.3 ± 2.4 Ma. This Hercynian age is interpreted as the time of crystallization of the magmatic (granitoid) protolith of the orthogneiss as a whole (see Fig. 4). Four analyses from the inherited oscillatory cores within the Hercynian crystals (similar to the one shown in Fig. 6b) gave analytically concordant ages between 593 ± 7 and 574 ± 7 Ma (Table 1).

The outermost—more or less oscillatory—thin rims surrounding the Hercynian cores were only in three cases broad enough to fit a SHRIMP spot. One of these three analyses, however, slightly touched the neighboring—older—igneous core domain, as indicated by post-SHRIMP CL studies (analysis number 55). The other two analyses yielded dates of 39.7 ± 1.2 and 38.1 ± 0.8 Ma (2σ errors). These dates are in agreement with the 40.0 ± 1.0 Ma age reported for the migmatization in Central Rhodope (Liati and Gebauer 1999). Therefore, it is very likely that the 39.7 ± 1.2 and 38.1 ± 0.8 Ma ages obtained here from the rims of the leucosome zircons correspond, also in West Rhodope, to the time of migmatization and leucosome formation (see below). This interpretation would also be in line with the oscillatory type of zoning observed in the rims surrounding the Hercynian cores, because oscillatory zoning is generally accepted to be characteristic of zircon precipitating in melts or fluids, also those forming the leucosomes.

Amphibolitized eclogite (no. RHO71)

Seventeen spots from the two different zircon domains (cores and rims) of this amphibolitized eclogite were analyzed (Table 1). Because the zircon cores are often crosscut by late fractures (e.g., Fig. 7b), it was difficult to find a suitable, i.e., fracture-free part of the magmatic cores to fit a SHRIMP spot. Thus, despite our efforts, most analyses included part of a fracture and show various amounts of Pb-loss (analyses number 59–64).

Three spots were analyzed in parts of the cores free of fractures. On a Terra–Wasserburg diagram, these three analyses define a mixing line between common Pb and a radiogenic $^{238}U/^{206}Pb$ end member intersecting the Concordia at an age of 245.6 ± 3.9 Ma (Fig. 12a), which is interpreted as the time of crystallization of the magmatic (gabbroic) protolith. A fourth analysis (Fig. 12a; uppermost dashed ellipse, closest to the mixing line) although sitting on a fracture, could also be included in the mixing line, together with the other three analyses considered above for the age calculation. This would yield an identical lower intercept age of 243.5 ± 7.8 Ma. However, the error is significantly larger and the MSWD value increases from 0.12 to 1.9. Therefore, it is preferred to take into account only the three analyses, as stated above.

One analysis from an inherited core yielded an analytically concordant age of 430 ± 7 Ma (Table 1).

Six analyses from the metamorphic zircon rims define a mixing line on a Terra–Wasserburg diagram intersecting the concordia at an age of 51.0 ± 1.0 Ma (Fig. 12b). This age is interpreted as being close to the time of HP metamorphism (see also REE geochemistry of zircon and interpretation of the results, Limitations of the metamorphic SHRIMP-ages and Geological implications sections).

As mentioned above (West Rhodope section), a euhedral, oscillatory zoned crystal was found among the zircons of this amphibolitized eclogite (Fig. 7c). One analysis on this crystal gave 38.1 ± 1.2 (2σ). Interestingly, this age fits rather well with the 39.7 ± 1.2 and 38.1 ± 0.8 Ma ages obtained from the oscillatory zoned fine rims of the adjacent migmatite leucosome zircons. It may be speculated, therefore, that this oscillatory zoned, euhedral zircon crystal grew entirely inside the leucosome melts or fluids of the migmatite and was then introduced into the adjacent amphibolitized eclogite in the form of small veinlets. Such veinlets are not obvious in the amphibolitized eclogite.

REE geochemistry of zircon and interpretation of the results

The REE composition of zircon depends on the concurrent growth of other REE-bearing minerals, which can be relevant for the identification of metamorphic conditions (for details on this issue see e.g., Rubatto 2002 and references therein; Hoskin and Schaltegger 2003 and references therein; Whitehouse and Platt 2003 and references therein). Such minerals, relevant for the present study are plagioclase, garnet and rutile. HP and (U)HP rocks do not contain plagioclase, which (together with K-feldspar) is the main sink for Eu. Therefore, its simultaneous growth with zircon results in Eu depletion of the latter mineral. As a consequence, a negative Eu anomaly appears in the chondrite-normalized REE pattern of zircon formed simultaneously with plagioclase. For rocks potentially containing plagioclase at low pressures, the lack of a Eu anomaly in the metamorphic domains of zircon would imply that these domains formed above the plagioclase stability field, that is under (U)HP conditions.

Regarding HREE, zircon generally displays HREE-enriched patterns (e.g., Hoskin and Ireland 2000).

Table 2 Trace and REE data of zircon from different rock types of the Rhodope zone, Northern Greece

Sample	La	Ce	Pr	Nd	Sm	Eu	Gd	Tb	Dy	Ho	Er	Tm	Yb	Lu	Y	Hf	Nb	Ta	Eu/Eu*
Garnet–kyanite metasediment (RHO65), Central Rhodope																			
Metamorphic rims																			
RHO65-6.1	0.172	0.802	0.056	0.231	0.311	0.252	3.281	1.044	8.672	1.817	5.315	0.857	7.511	1.262	63.30	10,793	ND	ND	0.482
RHO65-6.2	0.004	0.222	0.002	0.027	0.033	0.147	1.437	0.443	2.986	0.598	1.477	0.236	3.198	0.348	23.51	10,489	ND	ND	0.700
RHO65-7.2	0.002	0.553	0.005	0.071	0.098	0.228	2.380	0.706	4.900	0.870	2.058	0.328	3.721	0.312	29.77	12,683	ND	ND	0.641
RHO65-7.3	0.002	0.470	0.006	0.127	0.131	0.279	3.931	0.943	5.577	0.966	2.259	0.321	2.652	0.401	33.28	12846	ND	ND	0.481
Amphibolitized eclogite (RHO71), West Rhodope																			
Metamorphic rims																			
RHO71-2	< dl	0.085	< dl	< dl	0.059	0.056	1.101	0.505	5.150	1.248	4.372	0.823	6.766	1.245	50.10	95,371	0.487	0.154	0.336
RHO71-34	< dl	0.125	< dl	< dl	0.072	0.063	1.360	0.613	8.030	2.611	8.913	1.712	14.93	2.663	91.90	10,002	0.846	0.277	0.308
RHO71-30	< dl	0.086	< dl	< dl	< dl	0.083	0.958	0.627	7.072	1.786	6.078	1.145	6.900	1.124	65.88	10,299	0.585	0.298	0.526
RHO71-8	< dl	0.051	< dl	< dl	< dl	0.030	0.526	0.361	5.141	1.697	5.830	1.134	10.12	1.606	58.81	10,842	0.566	0.238	0.372
Igneous core																			
RHO71-23	2.558	39.09	4.203	6.937	49.59	4.440	231.0	537.7	1,053	1,938	2,877	3,703	5,260	6,443	2893.96	10,408	20.50	4.480	0.032
Amphibolitized kyanite eclogite (RHO1), Thermes area, Central Rhodope[a, b]																			
Metamorphic rims																			
RHO1-9.1	< dl	0.138	< dl	0.155	0.211	0.181	3.072	1.698	28.14	10.41	34.61	5.582	43.94	6.468	324.1	11,153	0.581	0.031	0.382
RHO1-9.2	0.014	0.142	< dl	< dl	0.105	0.231	3.201	1.878	29.04	11.06	35.16	5.529	41.30	6.475	334.8	11,072	0.493	0.045	0.488
RHO1-6.1	< dl	0.067	< dl	< dl	0.157	0.153	1.983	1.116	21.43	7.743	23.12	3.443	25.95	3.757	229.6	9,644	0.651	0.037	0.495

Notes: Data for sample RHO65 were obtained with SHRIMP II at the Australian National University, Canberra, for samples RHO71 and RHO1 with LA-ICPMS at ETH, Zurich < *dl* below detection limit, *ND* not determined, $Eu/Eu^* = Eu_n/(Sm_n + Gd_n)/2$, where Eu_n, Sm_n, Gd_n normalized to chondrite

[a] Liati and Seidel (1996)

[b] Liati and Gebauer (1999)

Garnet which is much more abundant incorporates also HREE, and its crystallization in a metamorphic environment results in a depletion of the reacting volume in HREE. As a result, simultaneously grown zircon would display a nearly flat or even negative HREE profile.

Rutile is, as a rule, the HP Ti-phase in rocks of basic composition (e.g., Hellman and Green 1979; Xiong et al. 2005 and references therein). It is a sink for Nb and Ta. Hence, low Nb and Ta contents in metamorphic zircon may be the result of concurrent growth of rutile (e.g., Li et al. 2005).

In the present work, REE analyses were performed on metamorphic rims of zircon crystals from both the grt–ky paragneiss of Central Rhodope (by SHRIMP II at ANU, Canberra), and from the amphibolitized eclogite of West Rhodope (by LA-ICPMS at ETH Zurich). In addition, metamorphic zircon domains of a previously dated amphibolitized kyanite eclogite from the area of Thermes, Central Rhodope (Figs. 2, 3) were included for REE analyses as well (LA-ICPMS). The metamorphic zircon domains of this amphibolitized kyanite eclogite show a SHRIMP-age of 42.2 ± 0.9 Ma, attributed to the time close to the HP metamorphic peak (Liati and Gebauer 1999). Knowledge of the REE composition of these zircon domains is important, as it can be used to support (or not) the link of the 42.2 ± 0.9 Ma age with HP metamorphism, with further implications for the geodynamic history. A detailed petrological study of the overprinted kyanite eclogite in Thermes area was already given by Liati and Seidel (1996).

The chondrite-normalized patterns determined for the metamorphic zircon domains of the three different rock types are illustrated in Fig. 13a–c and reveal the following features:

Garnet–kyanite paragneiss (RHO65), Central Rhodope The metamorphic rims of the analyzed zircons from this rock have very low Th/U ratios (< 0.004; Table 1) and only low trace and REE concentrations (Table 2) compared to igneous zircons (see e.g., Hoskin and Schaltegger 2003). No Eu anomaly or, in one case, a very weak one is observed in the REE pattern (Fig. 13a). This suggests the formation of zircon during metamorphism in the absence of plagioclase, probably above its stability field, and thus under—at least—HP conditions. The HREE profiles of zircon are flat. This feature is best explained by assuming zircon formation in the presence of garnet, probably even after substantial growth of garnet, since slightly negative slopes are observed as well.

Amphibolitized eclogite (RHO71), West Rhodope The metamorphic rims of the zircons analyzed from this rock type also have very low Th/U ratios (< 0.01; Table 1) and low trace and REE concentrations, as compared to the igneous cores (compare with analysis RHO71-23 in Table 2). La, Pr, Nd and, in two cases, Sm are below detection limit (dl) for LA-ICPMS (Table 2, Fig. 13b). For two samples with Sm < dl, (samples RHO71-30 and RHO71-8), the dl value has been plotted on the diagram as a maximum possible value (indicated by a down-pointing arrow in Fig. 13b). This was done because the concentration of Sm is critical for the identification of any Eu anomaly. Similar to the grt–ky paragneiss, the zircon rims of the amphibolitized eclogite show no Eu anomaly, thus indicating that they probably formed above the stability field of plagioclase. As shown in Fig. 13b, samples RHO71-30 and RHO71-8, for which the Sm contents were below dl, also exhibit no or only a very weak negative Eu anomaly, even considering a (maximum) Sm content equal to the dl. The REE pattern of an igneous zircon core (the one of Fig. 7a) is shown in Fig. 13b for comparison. The pattern of the core domain is characterized by much higher REE contents and a very pronounced negative Eu anomaly, consistent with the core crystallizing from a melt at a depth where plagioclase was stable. It is, therefore, evident that the absence or presence of a Eu anomaly is a distinctive feature to separate between igneous and later recrystallized HP zircon domains. HREE show flat (RHO71-30) or nearly flat profiles, compatible with the presence of garnet at the time of zircon formation. An interesting feature of the zircon rims is their low Nb and Ta contents, significantly lower than those of the igneous core (Table 2). As discussed before, this may be caused by simultaneous growth of rutile, thus providing an additional piece of evidence that these zircon domains are formed under HP conditions (see e.g., Li et al. 2005).

Amphibolitized kyanite eclogite (RHO1), Thermes area, Central Rhodope (Fig. 13c) The metamorphic domains of zircon from this rock have very low Th/U ratios (< 0.03). The trace and REE concentrations are a little higher than those of the metamorphic zircons of the amphibolitized eclogite of West Rhodope (Fig. 13b), but are much lower if compared to igneous zircons (e.g., igneous pattern of Fig. 13b; see also e.g., Hoskin and Ireland 2000). The REE profiles display no or a weak Eu anomaly, thus suggesting formation under high pressures. The HREE profile of the zircons is clearly flat, which is compatible with concurrent growth of garnet. Similar to the amphibolitized eclogite of West Rhodope, Nb and especially Ta contents are very low in the metamorphic zircon domains, consistent with a concurrent growth of rutile.

Limitations of the metamorphic SHRIMP-ages

The information provided by the REE spectra (REE geochemistry of zircon and interpretation of the results section), in combination with the CL-characteristics of the metamorphic zircon rims (Morphological charac-

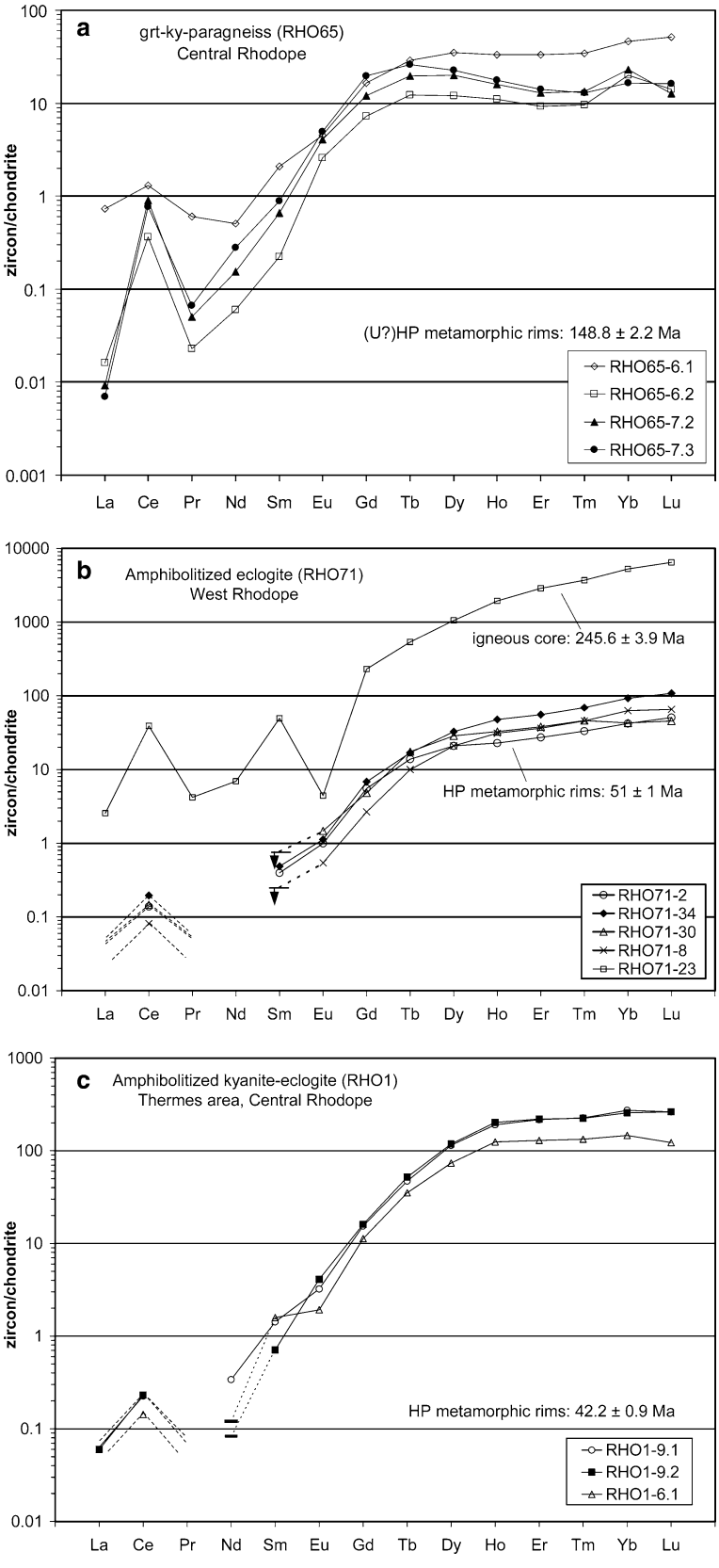

Fig. 13 Chondrite-normalized REE patterns of metamorphic zircon rims from the grt–ky paragneiss, Central Rhodope (RHO65 in **a**), the amphibolitized eclogite, West Rhodope (RHO71 in **b**) and an amphibolitized kyanite eclogite, Thermes area, Central Rhodope (RHO1 in **c**). In **b**, the pattern from an igneous zircon core is shown for comparison. Note the lack of Eu anomalies in all metamorphic zircon domains, (or a weakly negative Eu anomaly in one pattern of **c**) indicative of zircon formation under, at least, high pressures, as well as the flat HREE profiles reflecting more or less concurrent growth of garnet (see text). A pronounced negative Eu anomaly is shown in the igneous zircon core of (**b**), compatible with co-crystallization of plagioclase. Concentrations of La, Pr and Nd for all samples of (**b**) and (**c**) are not indicated in the diagram, because they are below dl (except for the magmatic core of **b**). In two cases, (RHO71-30 and RHO71-8), also Sm is below dl. In the latter case, the value plotted on the diagram is the maximum possible value (considering the dl value) and is indicated with a *down-pointing arrow* connected with a *dashed line* to Eu. Analyses RHO65-7.2 and −7.3 show a weak Yb-'peak'. These analyses were carried out in the same (SHRIMP II) sessions as all others and there is no difference with respect to mass stations counted at and interference peaks monitored. There was possibly either some sort of real effect or the accounting for the interferences does not apply for such compositions. Normalization values after Sun and McDonough (1989)

teristics and CL-imaging of zircon section), suggest that the metamorphic zircon domains of the grt–ky paragneiss (Central Rhodope) and the amphibolitized eclogite (West Rhodope) dated here, but also those of the amphibolitized kyanite eclogite (RHO1) dated in a previous study (Liati and Gebauer 1999) formed under—at least—HP conditions. It cannot be inferred, however, whether the metamorphic SHRIMP-ages reflect the peak of metamorphism or if they correspond to a stage shortly before or after the peak, within the (U)HP field. This is difficult to resolve, because HP and (U)HP metamorphic rocks are known for their high rates of burial as well as exhumation (e.g., Gebauer 1996; Gebauer et al. 1997; Amato et al. 1999; Rubatto and Hermann 2001 and references therein; Cartwright and Barnicoat 2002 and references therein). These rates may often exceed 1–2 cm/year (10–20 km/Ma), at least during part of their *P-T* path and thus fall into the depth uncertainties corresponding to the 95% cl errors of the SHRIMP-ages (compare also e.g., Liati and Gebauer 1999; Kröner et al. 2000; Rubatto and Hermann 2001; Hermann et al. 2001).

In the present study, the errors are on the order of 1.5–2%, referring to the 95% cl errors on the weighted mean ages. Thus, in the case of the 51.0 ± 1.0 Ma age obtained from the metamorphic zircon rims of the amphibolitized eclogite RHO71 (Table 1), for instance, the 1.0 Ma uncertainty on the age reflects also an uncertainty on the vertical distance covered by the rocks during subduction or exhumation at HP conditions. Assuming a subduction and/or exhumation (average) rate of 1–2 cm/year (10–20 km/Ma) for this rock, the ± 1.0 Ma error on the 51.0 Ma age would translate to an uncertainty of ± 10–20 km in depth (vertical distance). Consequently, for the (U)HP rocks of the upper tectonic unit of Rhodope dated here, it may suffice, in general, to state that SHRIMP-ages of the metamorphic zircon domains date subduction or exhumation events at (U)HP conditions. However, in certain cases, as in the area of Thermes, for instance, SHRIMP-ages of metamorphic zircon domains could be assigned to distinct metamorphic stages (Liati and Gebauer 1999; Liati et al. 2004). For comparison with the (U)HP rocks of the Dora Maira Massif, Western Alps, for instance, average exhumation rates of 2–2.4 cm/year (back to 10 km depth) were suggested by Gebauer et al. (1997); for their early stages of exhumation (between ca. 110 and 35 km) Rubatto and Hermann (2001) assumed faster rates, as much as 3.4 cm/year.

It is obvious that young (U)HP rocks show the lowest uncertainties in dating distinct stages of the metamorphic *P-T*-path because the absolute errors are—percentagewise—smallest. In the old (U)HP Kokchetav massif, for instance, metamorphic SHRIMP-ages of zircon, although they are documented to date different *P-T*-stages, show identical ages within error (527 ± 5, 528 ± 8 and 526 ± 5 Ma for the (U)HP stage, the granulite-facies overprint and the amphibolite-facies, respectively; Hermann et al. 2001).

Geological implications

Depositional ages

The only means to get information about sedimentation ages in rocks of high metamorphic grade, such as the metasedimentary grt–ky paragneisses of Central Rhodope, is to date detrital zircons, preserved in the form of 'cores' in composite zircon crystals and obtain a maximum time constraint for deposition. The youngest detrital zircon cores of the grt–ky paragneiss gave an Upper Proterozoic age of ca. 560 Ma (Table 1 and SHRIMP results section) implying that sedimentation started after Upper Proterozoic times. The absence of Hercynian detrital cores in the dated zircon grains of this paragneiss indicates that its sedimentation was possibly completed before erosion of any Hercynian rocks. Thus, the most likely deposition period for the sedimentary precursor of the grt–ky paragneiss can be bracketed between Upper Proterozoic and pre-Hercynian times. This time span holds true for the dated paragneiss but cannot be generalized for Central Rhodope. It is noted that sedimentation must have taken place also after ca. 300 Ma, as indicated by the presence of ca. 300 Ma old detrital zircon cores in calc-silicate gneisses, just north of the study area (close to Sminthi; Liati and Gebauer 2001b).

The age spectra of detrital zircons can be indicative of a potential provenance of the sediments. The common presence of 670–560 Ma and 2–2.1 Ga ages of the detrital zircon cores of the grt–ky paragneiss of Central Rhodope (Fig. 8), as well as the lack of 1.4–1.5 Ga-old cores (characteristic for Laurasia) argues for a Gondwana provenance of the eroded rocks (e.g., Gebauer 1993; Nance and Thompson 1996; Valverde-Vaquero et al. 2000 and references therein).

Magmatism

The Late Hercynian, ca. 295 Ma age obtained for the crystallization time of the granitoid protolith of the migmatized orthogneiss in West Rhodope (sample no. RHO21) is in line with previously reported Hercynian (ca. 300 Ma) magmatic ages in other areas of Rhodope (e.g., Thassos island: Wawrzenitz 1997; Central Rhodope, Thermes area: Liati and Gebauer 1999; East Rhodope, area of M. Derio: Liati and Fanning 2005; South Bulgaria: Peytcheva and von Quadt 1995). Thus, the presence of widespread Hercynian magmatism (so far found for granitoid rocks only) in this area of Europe is further supported by the present data.

The Late Permian/Early Triassic, ca. 245 age determined for the crystallization time of the gabbroic protolith of the amphibolitized eclogite (West Rhodope, sample no. RHO71) adjacent to above migmatites can suggest two possible alternative scenarios: (a) that these gabbroic rocks were part of a Late Permian/Early

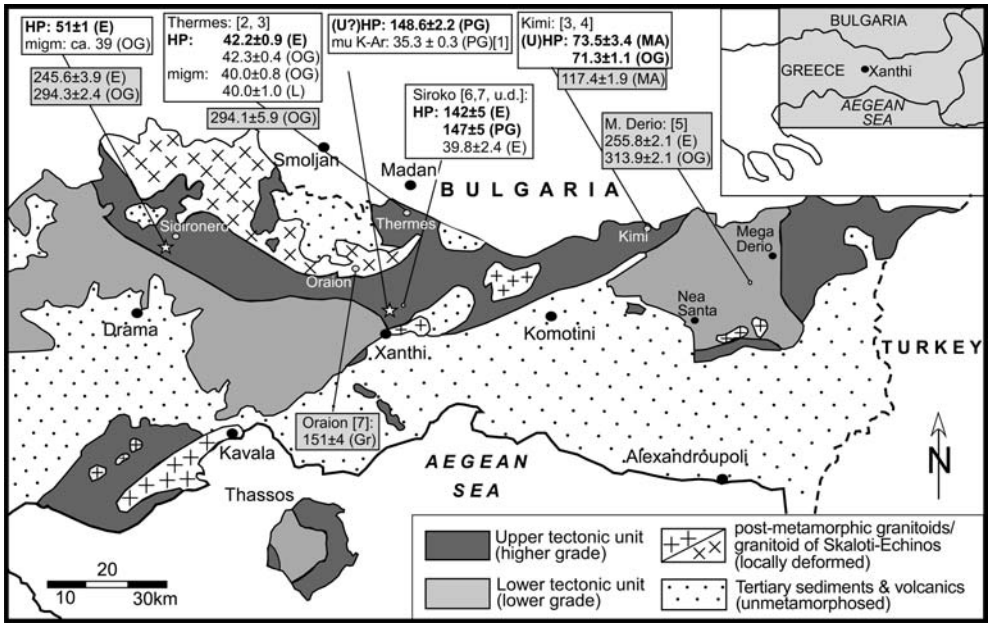

Fig. 14 Schematic map of Rhodope with the main tectonic units (based on Mposkos 1989), summarizing the radiometric (SHRIMP) data for the protoliths (*boxes with gray background*) and metamorphism (*boxes with white background*) of various rock types. The four different high- and/or ultra high-pressure events recorded in different areas are marked in *bold*. The *asterisks* indicate the locations of the samples dated in the present paper (north of Xanthi and north of Drama). Abbreviations: *E* amphibolitized eclogite, *OG* orthogneiss, *L* leucosome, *PG* paragneiss, *MA* grt-rich mafic rock, *Gr* deformed granitoid, *migm* migmatization, *u.d.* unpublished data. *1* Liati (1986), *2* Liati and Gebauer (1999), *3* Liati et al. (2004), *4* Liati et al. (2002), *5* Liati and Fanning (2005), *6* Liati and Gebauer (2001b), *7* Gebauer and Liati (1997). If no reference is given, the results are from the present study

Triassic ocean or (b) that they are related to underplating associated with Permo-Triassic rifting. The geochemistry of these metabasic rocks is in line with a MORB and partly IAT setting (Liati et al. 1990), which would be in favor of the first scenario. However, rock geochemistry may give only hints. The interpretation of geochemical data with respect to geotectonic setting is often disputable and should not be taken as an unquestionable argument. If the first scenario holds true, the gabbroic protolith of the amphibolitized eclogite of West Rhodope would be part of a Late Permian/Early Triassic branch of the Paleotethyan ocean. Similar crystallization ages of 255.8 ± 2.1 Ma were determined for metabasic rocks in the lower tectonic unit of East Rhodope, in the area west of Mega Derio (Fig. 14; Liati and Fanning 2005). It is also noted that this age has thus far been determined in the Rhodope only for rocks of basic composition.

Regarding the second scenario of a rift-related setting for the gabbroic protolith, it should be remembered that multi-episodic rifting in the Permian and Triassic is a common process throughout the Hercynian basement of western and central Europe (see e.g., Schaltegger and Gebauer 1999 for a review and references) and is often marked by the appearance of underplated mafic rocks. This could well be the case for the part of the Hercynian basement belonging to the Rhodope as well. So far, there are no clear arguments in favor of the first or the second scenario.

Finally, it might be of interest to add here that besides Hercynian magmatism, which is widespread in the Rhodope, Upper Jurassic magmatic activity seems to be also common: magmatic crystallization ages of 151 ± 4 Ma are recorded in zircons of a deformed granitoid rock (close to Oraion village; Fig. 3; Gebauer and Liati 1997) and in an orthogneiss in East Rhodope, Kimi area (150.4 ± 3.1 Ma; unpublished data). Identical ages of 151.9 ± 2.2 and 149 ± 0.7 Ma are also reported for the time of magmatic crystallization of an orthogneiss and a deformed porphyroclastic granite in the so-called Stratsevo unit and the Borovitsa unit of Bulgaria, respectively (NNE of Madan; Ovtcharova et al. 2004).

For a convenient survey of all the magmatic protoliths dated, these are shown within shaded boxes in the summarizing age map of Fig. 14.

Metamorphism

All metamorphic ages of the various parts of Rhodope as discussed in this paper are summarized in the age map of Fig. 14 and in the plot of Fig. 15. Details are being reported below in a geographic sequence:

Central Rhodope

SHRIMP-dating of metamorphic zircon domains from the grt–ky paragneiss in Central Rhodope (Table 1,

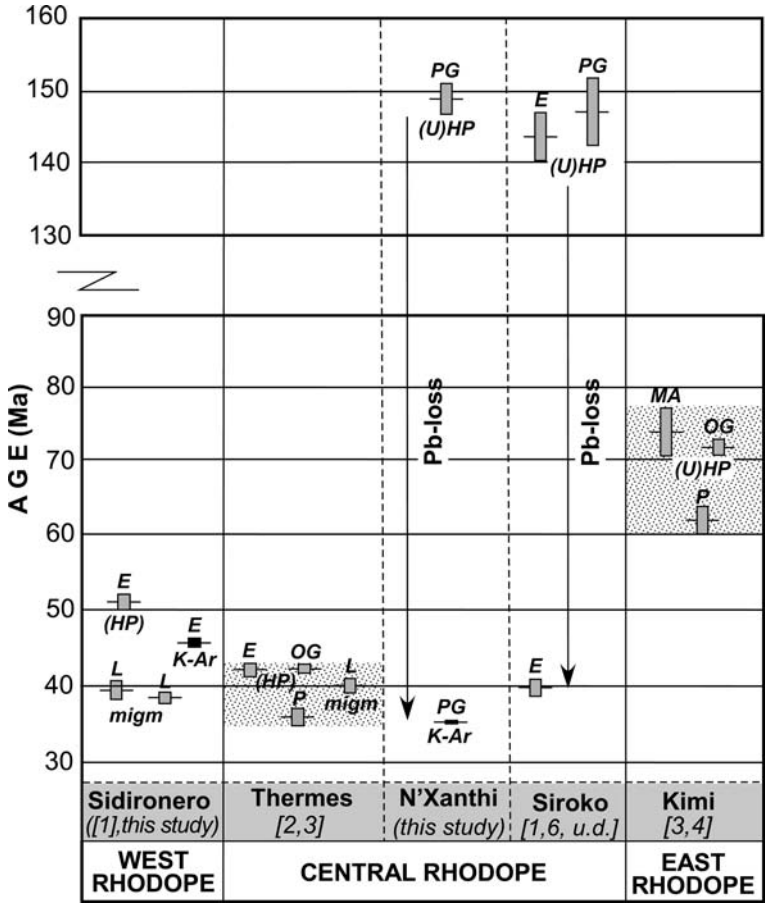

Fig. 15 Distribution of SHRIMP metamorphic ages of zircon from metamorphic rocks of the upper tectonic unit of West, Central and East Rhodope. The ages (*horizontal bars*) are given as lower intercept ages and the errors (*gray boxes*) at the 95% cl. Exceptions are the leucosome in West Rhodope, as well as the amphibolitized eclogite and the paragneiss of Siroko area (Central Rhodope), for which individual spot analyses with 2σ errors are illustrated (see text). Note Pb-loss in the areas Northern Xanthi (see also Fig. 10) and Siroko, which is probably connected to the influence of an Upper Eocene event (see text). In addition to the U–Pb SHRIMP zircon ages, K–Ar mineral data for two rock types are also given (*black boxes* marked K–Ar). The K–Ar data are from **a** muscovite of the grt–ky paragneiss of Central Rhodope and **b** hornblende of an amphibolitized eclogite of West Rhodope (only the youngest of scattered Alpine K–Ar hornblende data is shown; see text for details). For sample locations and different localities see map of Fig. 14. The *stippled fields* define the maximum range from the time close to the (U)HP-peak to the late stages of exhumation for the areas where it was determined (for Thermes and Kimi areas; see text). Abbreviations: *E* amphibolitized eclogite, *OG* orthogneiss, *L* leucosome, *PG* paragneiss, *P* pegmatite, *MA* garnet-rich mafic rock, *migm* migmatization, *HP* high-pressure, *(U)HP* (ultra) high-pressure. *1* Liati (1986), Liati and Kreuzer (1990); *2* Liati and Gebauer (1999); *3* Liati et al. (2004); *4* Liati et al. (2002); *6* Liati and Gebauer (2001b); *u.d.* unpublished data

numbers 18–29) revealed that this rock has been affected by a Late Jurassic (148.8 ± 2.2 Ma) metamorphic event involving high or ultrahigh pressures (see REE geochemistry of zircon and interpretation of the results, Limitations of the metamorphic SHRIMP-ages sections). K–Ar muscovite data of 35.3 ± 0.3 Ma were reported for the same grt–ky paragneisses (Liati 1986; Liati and Kreuzer 1990). These and other Upper Eocene K–Ar data by the above authors in this area probably mark the late stages of a metamorphic event at that time (see also Previous geochronology of metamorphic rocks in the Rhodope section). A 36.1 ± 1.2 Ma SHRIMP zircon age obtained for a pegmatite crosscutting the metamorphic rocks, just north of the area studied here, was interpreted as dating the late stages of an Upper Eocene metamorphic event (Liati and Gebauer 1999). This Upper Eocene event reached HP, at least in the northern part of Central Rhodope (area of Thermes, Fig. 14; Liati and Gebauer 1999; Liati et al. 2004). Thus, the grt–ky paragneiss went possibly through two distinct metamorphic cycles: one at 148.8 ± 2.2 Ma [HP or (U)HP] and a second one ending at ca. 35–36 Ma (Fig. 15). This inference is in line with the post-Upper Jurassic zircon data of the same grt–ky paragneiss showing variable Pb-loss (Fig. 10), attributed here to a metamorphic/fluid event post-dating the (U)HP Upper Jurassic metamorphism. It is not clear as to whether or not the grt–ky paragneiss underwent HP metamorphism during the second (Upper Eocene) metamorphic cycle as well.

The Upper Jurassic metamorphic event identified here by SHRIMP in the grt–ky paragneisses of Central

Rhodope does not seem to be restricted only to this rock type. Metamorphic zircon domains of amphibolitized eclogites and their country rock paragneisses in the area of Siroko (Figs. 14, 15) record also Upper Jurassic (SHRIMP) ages (Gebauer and Liati 1997; Liati and Gebauer 2001b; Liati and Gebauer, unpublished data): the oldest of a series of (geologically) discordant data with various amounts of Pb-loss are 143.4 ± 3.3 Ma (amphibolitized eclogite) and 147.2 ± 4.7 Ma (paragneiss) (1σ errors). The chondrite-normalized REE patterns of the 143.4 ± 3.3-Ma-old metamorphic zircon domains of the amphibolitized eclogite in Siroko show no Eu anomaly (Liati et al. 2005a), which supports the view that these metamorphic zircon domains formed at HP. The youngest dates obtained in metamorphic zircon domains of the same amphibolitized eclogites are 39.8 ± 2.4 Ma (1σ; Fig. 15). Thus, similar to the grt–ky paragneisses, the amphibolitized eclogites of Siroko area seem to have undergone, together with their country rocks, two metamorphic events: an Upper Jurassic event (of at least HP) and a Late Eocene one. The Upper Jurassic metamorphic event in Central Rhodope and the Upper Jurassic magmatic activity inferred from the protolith (granitoid) ages of a number of orthogneisses (see Magmatism) probably belong to the same orogenic cycle.

West Rhodope

In West Rhodope, the 51 ± 1 Ma event attributed here to a HP metamorphic stage (see Limitations of the metamorphic SHRIMP-ages section and Figs. 14, 15) is identified only in the amphibolitized eclogites but not in the adjacent migmatites. The leucosome zircons of these migmatites show rare and fine oscillatory zoned ca. 39 Ma old overgrowths around Hercynian magmatic crystals (Fig. 6a, c). The ca. 39 Ma age of these overgrowths is interpreted here as the time of leucosome formation during migmatization (see above). It is, therefore, likely that these migmatized orthogneisses have not been metamorphosed together with the adjacent eclogites at high pressures; at least they do not preserve any petrological or geochronological evidence of HP metamorphism. The two rock types (the migmatized orthogneiss and the amphibolitized eclogite) may have come together tectonically, after the 51 Ma, HP event. The presence of a 38.1 ± 1.2 Ma old newly formed oscillatory zircon among the 51 Ma old metamorphic zircons of the amphibolitized eclogite indicates that this zircon could have possibly precipitated within a veinlet crosscutting the eclogite. Such a veinlet may be genetically related to the leucosome formation (sample RHO21) and migmatization processes in the adjacent orthogneiss (see above, West Rhodope section). It may be worth mentioning that zircons from migmatized orthogneisses in the area of Thermes, Central Rhodope, have broad metamorphic rims, which show the same HP metamorphic SHRIMP-age of ca. 42 Ma as the enclosed eclogites (eclogites: 42.2 ± 0.9 Ma; migmatized orthogneisses: 42.3 ± 0.4 Ma; Liati and Gebauer 1999; Liati et al. 2004). This is at variance with the migmatized orthogneisses of West Rhodope, which do not record the 51 ± 1 (HP age) of the adjacent amphibolitized eclogites but only show ca. 39 Ma old thin rims with oscillatory zoning associated with migmatization (see also Fig. 15).

K–Ar hornblende data of amphibolitized eclogites from the same area of West Rhodope scatter widely between 45.6 ± 0.7 and 81.0 ± 1.5 Ma (Liati 1986; Liati and Kreuzer 1990). Although these K–Ar data are relatively inconclusive (see Previous geochronology of metamorphic rocks in the Rhodope section), they are indicative of an Upper Eocene metamorphic event, possibly younger than the youngest K–Ar hornblende date (45.6 ± 0.7 Ma). The ca. 39 Ma SHRIMP-age of the leucosome zircon rims (Table 1, sample RHO21, number 53, 54) attributed here to migmatization, in combination with the above K–Ar data, imply that the Upper Eocene metamorphic event, which is widespread in Central Rhodope (see above) affected also rocks of West Rhodope.

East Rhodope

In East Rhodope, the time of (U)HP metamorphism is different from both Central and West Rhodope (Fig. 15): a metamorphic event at ca. 73 Ma, determined for two different rock types (garnet-rich mafic rock: 73.5 ± 3.4 Ma; orthogneiss: 71.3 ± 1.1 Ma), was interpreted to reflect (U)HP metamorphism (SHRIMP-data on zircon; Liati et al. 2002, 2004). The REE pattern of the 73.5 ± 3.4 Ma old metamorphic zircon domains shows complete lack of Eu anomaly, supporting (U)HP conditions (Liati et al. 2004, 2005a). The late stages of this metamorphic cycle occurred at 61.9 ± 1.9 Ma (Fig. 15), as indicated by the age of newly formed zircons in pegmatoids crosscutting the metamorphic rocks (Liati et al. 2002).

Concluding remarks

Summarizing the data reported above and in Figs. 14 and 15, four distinct metamorphic events can be distinguished in possibly different tectonometamorphic units of Rhodope during Alpine times:

- At ca. 149 Ma: (U)HPM in two areas of Central Rhodope lying close by, North of Xanthi,
- At ca. 73 Ma: (U)HPM in East Rhodope, Kimi area,
- At ca. 51 Ma: HPM in West Rhodope, Sidironero area, and
- At ca. 42 Ma: HPM in the Thermes area of Central Rhodope.

Obviously, the extent of these different units and their exact boundaries still need to be determined, on the basis of tectonic data and more geochronological and petrological information. It needs to be stressed also that the

ca. 42 Ma metamorphic cycle, ending at ca. 36 Ma, is probably quite widespread at least in Central and West Rhodope (see also Previous geochronology of metamorphic rocks in the Rhodope section and Figs. 14, 15). However, so far only in Thermes it could be connected with high pressures.

Identification of four different (U)HP metamorphic events in four different regions of Rhodope can be explained by assuming the former existence of different crustal fragments within a long-term compressional environment. It may thus be suggested here that the Rhodope consists of a puzzle of different terranes, which resulted from multiple subduction and collision cycles of different crustal fragments (microcontinents) squeezed between the two major plates of Africa and Europe, in the course of Alpine convergence. These microcontinents had possibly been rifted off from thinned continental margins of Gondwana. Future multidisciplinary studies in terms of geochronological but also structural and petrological data are expected to better clarify and complete our understanding of the geodynamic evolution of the Rhodope.

Comparing the present state of knowledge in the Rhodope with that of the Alps, it might be worth remembering that up to about 15 years ago, a model for Alpine geodynamics existed which assumed one single, long-lasting subduction–exhumation cycle for the Western and Central European Alps (from ca. 140 to 30 Ma; see e.g., summary by Hunziker et al. 1992). This had to be abandoned mainly after application of a detailed CL-controlled SHRIMP geochronology. It was more and more confirmed since, also in other (U)HP orogenic belts worldwide, that such long durations are unrealistic for single (U)HP metamorphic cycles (e.g., Gebauer 1996; Gebauer et al. 1997; Amato et al. 1999; Rubatto and Hermann 2001 and references therein). Thus, for the Central and Western Alps, a very different model involving multiple subductions of different terranes at different Alpine times was suggested on the basis of SHRIMP-data, combined with a detailed structural, geological and petrological information (see e.g., summary by Gebauer 1999; Froitzheim 2001; Liati et al. 2005b and references therein). Four distinct Alpine cycles are envisaged so far for the Western and Central Alps involving subduction/collision of different oceanic and continental fragments at ca. 65, 44, 39 and 35 Ma.

The data presented and summarized in the present work can be regarded as an attempt of a preliminary subdivision of the Rhodope into distinct terranes, which underwent different metamorphic cycles at different Alpine times, in analogy to the model for the European Western and Central Alps.

Acknowledgments M. Hamilton, R. Stern, N. Rayner and W. Davis, GSC, Ottawa, as well as M. Fanning, RSES, ANU Canberra are gratefully acknowledged for their valuable help during various stages of SHRIMP analytical work and data evaluation. Many thanks to D. Gebauer, ETH Zurich, for his help in the field, for numerous constructive discussions and for useful remarks on the manuscript. The help of Th. Pettke, ETH Zurich, during the LA-ICPMS REE analyses is greatly appreciated. Thanks are due to D. Rubatto, Canberra and an anonymous reviewer for their comments and suggestions. I very much appreciate the help of W. Schreyer, Bochum, not only concerning the editorial support but also his constructive comments, which led to significant improvement of the manuscript. This study was supported by a grant from the Swiss National Science Foundation (20-63767.00).

References

Amato JM, Johnson CM, Baumgartner L, Beard BL (1999) Rapid exhumation of the Zermatt-Saas ophiolite deduced from high-precision Sm–Nd and Rb–Sr geochronology. Earth Planet Sci Lett 171:425–438

Beyssac O, Chopin Ch (2003) Comment on: "Diamond, former coesite and supersilicic garnet in metasedimentary rocks from the Greek Rhodope: a new ultrahigh-pressure metamorphic province established." by E. Mposkos and D. Kostopoulos. Earth Planet Sci Lett 214:669–674

Burchfiel BC (1980) Eastern European Alpine system and the Carpathian orocline as an example of collision tectonics. Tectonophysics 63:31–61

Burg J-P, Ivanov Z, Ricou L-E, Dimor D, Klain L (1990) Implications of shear-sense criteria for the tectonic evolution of the Central Rhodope massif, southern Bulgaria. Geology 18:451–454

Burg J-P, Godfriaux I, Ricou LE (1995) Extension of the Mesozoic Rhodope thrust units in the Vertiskos-Kerdyllion Massifs (Northern Greece). CR Acad Sci Paris t 320, série II a, pp 889–896

Burg J-P, Ricou LE, Ivanov Z, Godfriaux I, Dimov D, Klain L (1996) Syn-metamorphic nappe complex in the Rhodope Massif. Structure and kinematics. Terra Nova 8:6–15

Cartwright I, Barnicoat AC (2002) Petrology, geochronology and tectonics of shear zones in the Zermatt-Saas and Combin zones of the Western Alps. J Metam Geol 20:263–281

Chatzipanagis I (1991) The geologic structure of the broad area of Falakron mountain. PhD Thesis, National Technical University of Athens, pp 179

Compston W, Williams IS, Kirschvink JL, Zichao Z, Guogan MA (1992) Zircon U–Pb ages for the Early Cambrian time-scale. J Geol Soc Lond 149:171–184

Cumming GL, Richards GR (1975) Ore lead isotope ratios in a continuously changing Earth. Earth Planet Sci Lett 28:155–171

Dinter DA, Royden L (1993) Late Cenozoic extension in northeastern Greece: Strymon valley detachment system and Rhodope metamorphic core complex. Geology 21:45–48

Dinter DA, Macfarlane A, Hames W, Isachsen C, Bowring S, Royden L (1995) U–Pb and $^{40}Ar/^{39}Ar$ geochronology of the Symvolon granodiorite: implications for the thermal and structural evolution of the Rhodope metamorphic core complex, northeastern Greece. Tectonics 14:886–908

Franz G, Thomas S, Smith DC (1986) High pressure phengite decomposition in the Weissenstein eclogite, Münchberg Gneiss Massif, Germany. Contrib Mineral Petrol 92:71–87

Froitzheim N (2001) Origin of the Monte Rosa nappe in the Pennine Alps—a new working hypothesis. Geol Soc Am Bull 113:604–614

Gebauer D (1993) The Pre-Alpine evolution of the continental crust of the Central Alps–an overview. In: von Raumer JF, Neubauer F (eds) Pre-mesozoic geology in the alps. Springer, Berlin Heidelberg New York, pp 93–117

Gebauer D (1996) A P–T–t path for a (ultra?) high-pressure ultramafic/mafic rock associations and their felsic country-rocks based on SHRIMP-dating of magmatic and metamorphic zircon domains. Example: Alpe Arami (Central Swiss Alps). In: Earth processes: reading the isotopic code; Special AGU-monograph. Geophys Monogr 95:307–329

Gebauer D (1999) Alpine geochronology of the Central and Western Alps: new constraints for a complex geodynamic evolution. Schweiz Mineral Petrogr Mitt 79:191–208

Gebauer D, Liati A (1997) Geochronological evidence for Mesozoic rifting and oceanization followed by Eocene subduction in the Rhodope Complex (Northern Greece). Terra Nova 9(Abstract supplement 1):10

Gebauer D, Schertl HP, Brix M, Schreyer W (1997) 35 Ma old ultrahigh-pressure metamorphism and evidence for very rapid exhumation in the Dora Maira Massif, Western Alps. Lithos 41:5–24

Heinrich CA (1982) Kyanite-eclogite to amphibolite-facies evolution of hydrous mafic and pelitic rocks, Adula nappe, Central Alps. Contrib Mineral Petrol 81:30–38

Heinrich CA (1986) Eclogite facies regional metamorphism of hydrous mafic rocks in the Central Alpine Adula nappe. J Petrol 27:123–154

Hellman PL, Green TH (1979) The role of sphene as an accessory phase in the high pressure partial melting of hydrous mafic compositions. Earth Planet Sci Lett 42:191–201

Hermann J, Rubatto D, Korsakov A, Schatsky VS (2001) Multiple zircon growth during fast exhumation of diamondiferous, deeply subducted continental crus (Kokchetav massif, Kazakhstan) Contrib Mineral Petrol 141:66–82

Hoskin PWO (1998) Minor and trace element analysis of natural zircon ($ZrSiO_4$) by SIMS and laser ablation ICPMS: a consideration and comparison of two broadly competitive techniques. J Trace Microprobe Techn 16:301–306

Hoskin PWO, Ireland TR (2000) Rare earth element chemistry of zircon and its uses as a provenance indicator. Geology 28:627–630

Hoskin PWO, Schaltegger U (2003) The composition of zircon and igneous and metamorphic petrogenesis. In: Hanchar MJ, Hoskin PWO (eds) Zircon, vol 53. Reviews in Mineralogy and Geochemistry, pp 27–62

Hunziker JC, Desmons J, Hurford AJ (1992) Thirty-two years of geochronological research in the Central and Western Alps: a review on seven maps. Mém Géol (Lausanne) 13:1–59

Ivanov Z (2000) ABCD GEODE workshop—Borovets, excursion guide B, pp 50

Jones C, Tarney J, Barreiro B (1994) The make-up and melting of a subduction-accretion complex: generation of S- and I-type granitoids. Abstracts of the 8th international conference on Geochr Cosmochr and Isotope Geol, Berkeley, pp 160

Kelley S (2002) Excess argon in K–Ar and Ar–Ar geochronology. Chem Geol 188:1–22

Kolceva K, Zeljaskova-Panajotova M, Bobrecov NL, Stojanova V (1986) Eclogites in Central Rhodope metamorphic group and their retrograde metamorphism. Geochem Mineral Petrol (Sofia) 20(21):130–144

Koons PO, Thompson AB (1985) Non-mafic rocks in the greenschist, blueschist and eclogite facies. Chem Geol 50:3–30

Kröner A, O'Brien PJ, Nemchin AA, Pidgeon RT (2000) Zircon ages for high pressure granulites from South Bohemia, Czech Republic, and their connection to Carboniferous high temperature processes. Contrib Mineral Petrol 138:127–142

Li QL, Li SG, Hou ZH, Hong J, Yang W (2005) A combined study of SHRIMP U-Pb dating, trace element and mineral inclusions on high-pressure metamorphic overgrowth zircon in eclogite from Qinglongshan in the Sulu terrane. Chin Sci Bull 50:459–465

Liati A (1986) Regional metamorphism and overprinting contact metamorphism of the Rhodope zone, near Xanthi, N. Greece: petrology, geochemistry, geochronology. Dissertation, Techn Univ Braunschweig, pp 186

Liati A, Fanning CM (2005) Eclogites and their country rock orthogneisses in East Rhodope representing Upper Permian gabbros and Upper Carboniferous granitoids: Geochronological constraints. Mitt Oesterr Mineral Ges 150:88

Liati A, Gebauer D (1999) Constraining the prograde and retrograde P–T–t path of Eocene HP-rocks by SHRIMP dating of different zircon domains: inferred rates of heating, burial, cooling and exhumation for central Rhodope, northern Greece. Contrib Mineral Petrol 135:340–354

Liati A, Gebauer D (2001a) Alpine UHP rocks in the Rhodope zone (N' Greece): evidence from exsolution textures in garnet-rich rocks. In: Proceedings of the 6th international eclogite conference, Abstract volume, pp 76–77

Liati A, Gebauer D (2001b) Palaeozoic as well as Mesozoic sedimentation and polymetamorphism in Central Rhodope (N' Greece) as inferred from U–Pb SHRIMP-dating of detrital zircons. EUG 11, Journal of Conference Abstracts 6:315

Liati A, Kreuzer H (1990) K–Ar dating of metamorphic and magmatic rocks from the Xanthi and Drama areas, Greek part of the Rhodope zone. Eur J Mineral 2(Bh 1):161

Liati A, Seidel E (1996) Metamorphic evolution and geochemistry of kyanite eclogites in central Rhodope, N' Greece. Contrib Mineral Petrol 123:293–307

Liati A, Mposkos E, Perdikatsis V (1990) Geochemical constraints on the nature and tectonic setting of the metabasite protoliths from the Rhodope zone, N. Greece. Eur J Mineral 2(Bh 1):162

Liati A, Gebauer D, Wysoczanski R (2002) U–Pb SHRIMP-dating of zircon domains from UHP mafic rocks in the Rhodope zone (N' Greece); evidence for Early Cretaceous crystallization and Late Cretaceous metamorphism. Chem Geol 184:281–300

Liati A, Gebauer D, Fanning CM (2004) The duration of exhumation processes in (U)HP terranes—a geochronological approach applied to the Rhodope terrane, N' Greece. 'Geoscience Africa 2004', The Birth and Growth of Continents, Abstract volume 1:384–385

Liati A, Pettke T, Fanning CM (2005a) Linking U–Pb SHRIMP zircon ages with metamorphic conditions: constraints from the REE composition of zircon in Alpine (U)HP rocks of the Rhodope, N' Greece. Mitt Oesterr Mineral Ges 150:90

Liati A, Froitzheim N, Fanning MC (2005b) Jurassic ophiolites within the Valais domain of the Western and Central Alps: geochronological evidence for re-rifting of oceanic crust. Contrib Mineral Petrol 149:446–461

Lips ALW, White SH, Wijbrans JR (2000) Middle-Late Alpine thermotectonic evolution of the southern Rhodope Massif, Greece. Geodinam Acta 13:281–292

Ludwig K (2000) User's manual for Isoplot/Ex, version 2.4. A geochronological toolkit for microsoft excel. Berkeley Geochronological Center, Special Publication No. 1a, pp 53

Mposkos E (1989) High-pressure metamorphism in gneisses and pelitic schists in East Rhodope zone (N Greece). Mineral Petrol 41:337–351

Mposkos E (1994) Metamorphic evolution of the lower and upper tectonic unit of Rhodope: similarities and differences. Bull Geol Soc Greece 23(1):255–267

Mposkos E, Liati A (1993) Metamorphic evolution of metapelites in the high pressure terrain of Rhodope, N. Greece. Can Mineral 31:401–424

Mposkos E, Liati A, Katagas Ch, Arvanitides N (1990) Petrology of the metamorphic rocks of Western Rhodope, Drama area, N Greece. Geol Rhodopica 2:127–142

Mposkos E, Wawrzenitz N (1995) Metapegmatites and pegmatites bracketing the time of HP-metamorphism in polymetamorphic rocks of the E-Rhodope, N. Greece: petrological and geochronological constraints. Geol Soc Greece Sp Publ 4(2):602–608

Mposkos E, Kostopoulos D (2001) Diamond, former coesite and supersilicic garnet in metasedimentary rocks from the Greek Rhodope: a new ultrahigh-pressure metamorphic province established. Earth Planet Sci Lett 192:497–506

Nakamura D (2003) Stability of phengite and biotite in eclogites and characteristics of biotite- or orthopyroxene-bearing eclogites. Contrib Mineral Petrol 145:550–567

Nance RD, Thompson MD (1996) Avalonian and related peri-Gondwanan terranes of the circum-North Atlantic. GSA Spec Paper 304, pp 390

Ovtcharova M, von Quadt A, Heinrich CA, Frank M, Kaiser-Rohrmeier M (2003) Triggering of hydrothermal ore mineralization in the Central Rhodopean Core Complex (Bulgaria)—insight from isotope and geochronological studies on

tertiary magmatism and migmatization. In: Eliopoulos D et al (eds) Mineral exploration and sustainable development, Millpress, pp 367–370
Ovtcharova M, von Quadt A, Cherneva Z, Sarov S, Heinrich CA, Peytcheva I (2004) U–Pb dating of zircon and monazite from grantoids and migmatites in the core and eastern periphery of the Central Rhodopean Dome, Bulgaria. Conference Supplement of Geochim Cosmochim Acta, pp A664
Papanikolaou D, Panagopoulos G (1981) On the structural style of Southern Rhodope (Greece). Geol Balc 11:13–22
Pettke T, Halter WE, Webster JD, Aigner-Torres M, Heinrich CA (2004) Accurate quantification of melt inclusion chemistry by LA-ICPMS: a comparison with EMP and SIMS and advantages and possible limitations of these methods. Lithos 78:333–361
Peytcheva I, von Quadt A (1995) U–Pb zircon dating of metagranites from Byala Reka region in the East Rhodopes, Bulgaria. Geol Soc Greece Sp Publ., No. 4, 2:637–642
Rohrmeier M, von Quadt A, Handler R, Ovtcharova M, Ivanov Z, Heinrich CA (2002) The geodynamic evolution of hydrothermal vein deposits in the Madan metamorphic core complex, Bulgaria. Geochim Cosmochim Acta 66(S1):A645
Rubatto D (2002) Zircon trace element geochemistry: partitioning with garnet and the link between U–Pb ages and metamorphism. Chem Geol 184:123–138
Rubatto D, Hermann J (2001) Exhumation as fast as subduction? Geology 29:3–6
Rubatto D, Liati A, Gebauer D (2003) Dating UHP metamorphism. EMU Notes in Mineralogy 5:341–363
Schaltegger U, Gebauer D (1999) Pre-Alpine geochronology of the Central, Western and Southern Alps. Schweiz Mineral Petrogr Mitt 79:79–87
Sommerauer J (1974) Trace elements distribution patterns and mineralogical stability of zircons—an application for combined electron microprobe techniques. Electron Microscopy Society of Southern Africa, Proceedings 4:71–72
Stern RA (1997) The GSC sensitive high resolution ion microprobe (SHRIMP): analytical techniques of zircon U–Th–Pb age determinations and performance evaluation. In: Radiogenic Age and Isotopic Studies: Report 10; Geological Survey of Canada, Current Research, 1–31
Sun SS, McDonough WF (1989) Chemical and isotopic systematics of oceanic basalts: implications for mantle composition and processes. In: Sanders AD, Norry MJ (eds) Magmatism in the ocean basins, vol 42. Geol Soc London Special Publication, pp 313–345
Tera F, Wasserburg GJ (1972) U–Th–Pb systematics in three Apollo 14 basalts and the problem of initial Pb in lunar rocks. Earth Planet Sci Lett 14:281–304
Tilton GR, Ames L, Schertl HP, Schreyer W (1997) Reconnaissance isotopic investigations on rocks of an undeformed granite contact within the coesite-bearing unit of the Dora Maira Massif. Lithos 41:25–36
Valverde-Vaquero P, Dörr W, Belka Z, Franke W, Wiszniewska J, Schastok J (2000) U–Pb single-grain dating of detrital zircon in the Cambrian of central Poland: implications for Gondwana versus Baltica provenance studies. Earth Planet Sci Lett 184:225–240
Villa I (1998) Isotopic closure. Terra Nova 10:42–47
Wawrzenitz N (1997) Mikrostrukturell unterstützte Datierung von Deformationsinkrementen in Myloniten: Dauer der Exhumierung und Aufdomung des metamorphen Kernkomplexes der Insel Thassos (Süd-Rhodope, Nordgriechenland). Dissertation, Universität Erlangen, pp 192
Whitehouse M, Platt J (2003) Dating high-grade metamorphism–constraints from rare earth elements in zircon and garnet. Contrib Mineral Petrol 145:61–74
Williams IS (1998) U–Th–Pb Geochronology by Ion Microprobe. In: McKibben MA, Shanks WC III, Ridley WI (eds) Applications of microanalytical techniques to understanding mineralizing processes. Reviews in Economic Geology 7:1–35
Williams IS, Buick S, Cartwright I (1996) An extended episode of early Mesoproterozoic metamorphic fluid flow in the Reynolds Range, central Australia. J Metam Geol 14:29–47
Xiong XL, Adam J, Green TH (2005) Rutile stability and rutile/melt HFSE partitioning during partial melting of hydrous basalt: implications for TTG genesis. Chem Geol 218:339–359
Yang TN, Xu ZQ, Leech M (2004) Mass balance during retrogression of eclogite-facies minerals in the Rongcheng eclogite, eastern Sulu ultrahigh-pressure terrane, China. Am Mineral 89:1525–1532